Sensitivity to climate change of the thermal structure and ice cover regime of three hydropower reservoirs

Solomon Gebre, *Thibault Boissy and Knut Alfredsen

Department of Hydraulic and Environmental Engineering

Norwegian University of Science and Technology

NO-7491 Trondheim, Norway

Corresponding author:

Solomon Gebre

Department of Hydraulic and Environmental Engineering

Norwegian University of Science and Technology

S.P. Andersens Veg 5

NO-7491 Trondheim, Norway

E-mail: Solomon.gebre@ntnu.no

Tel: +47 94789120

* Present Address:

Conseil Général de la Savoie

l'Adret

1 rue des Cévennes

73000 CHAMBÉRY-LE-HAUT

ABSTRACT

This study examines the effect of climate-induced changes on the thermal state and ice cover regime of three reservoirs in Norway: Tesse, Follsjoe and Alta. The model used for the task is *MyLake* which is a one-dimensional deterministic model for lake ice and thermal stratification, which we modified to handle the effects of reservoir outflows. The model was first validated using observational datasets and it reproduced the vertical temperature profiles of the reservoirs, the withdrawal temperatures, and the ice cover dynamics reasonably well. The mean absolute error for vertical temperature predictions ranged from 0.7 ^{o}C to 1.13 ^{o}C. The validated model was then applied to investigate the impacts of climate change on the ice cover regime, the seasonal temperature profiles in general and the withdrawal water temperatures in particular. The climate change model forcings come from the medium level emission scenario A1B and two global circulation models (GCMs), which are dynamically downscaled using a regional climate model (RCM). Some of the predicted effects of climate change include: a reduction in ice cover duration ranging between 15 to 44 days in 2050s and 27 to 81 days in 2080s, depending on the scenarios and hydro-climatic conditions of the reservoirs. As a consequence of this, the period of stratification is lengthened by 20 to 31 days in 2050s, and 22 to 36 days in 2080s. The results also revealed that the southern near coastal reservoir (Follsjoe) is much more sensitive to the climate change signals compared to the inland (Tesse) and arctic (Alta) reservoirs.

Key words: *MyLake*, one-dimensional model, thermal stratification, ice cover, reservoir, climate change.

1 INTRODUCTION

Creating reservoirs on rivers or regulating natural lakes for various uses lead to physical, chemical, and biological alterations in the rivers downstream and the lakes/reservoirs themselves (Collier et al., 1996; Wetzel, 2001a). One of the physical alterations of reservoir operation is its influence on the in-reservoir thermal stratification as well as the temporal flow and thermal regimes downstream (Baxter, 1977; Bevelhimer et al., 1997; Collier et al., 1996; Jager and Smith, 2008). The largest temperature changes in Norwegian rivers, for example, are linked to the outflows from the deep mountain reservoirs. Temperatures in rivers downstream power plants fed by these reservoirs are 1 to 5 °C lower in mid-summer and 0.5 to 2 °C higher in winter than before the regulation (Saltveit, 2006).

Thermal and density stratification is a phenomenon that occurs in almost all lakes and reservoir impoundments in cold regions (Imberger, 1982). The thermodynamics and ice cover dynamics of a freshwater lake or reservoir are governed by meteorological forcings that determine the surface heat flux and the inflows and outflows of water (Henderson-Sellers, 1986), which are all in turn dependent on climatic conditions. A reservoir is essentially different from a natural lake due to the complexity associated with dynamic outflows (Fischer et al., 1979). That is, water level changes are more dynamic in the case of reservoirs than natural lakes. Hence, the vertical movement of the water mass and the advective heat transfer as a result can play an important role in the distribution of water temperature (Arai, 1973), and possibly on the ice cover dynamics. Generally, because of vertical mixing due to water withdrawal, the temperature in the summer season in the deep layer of the reservoir becomes higher than that of a natural lake at the same depth (Arai, 1973; Ford and Johnson, 1986). The reverse of this can happen in winter as the colder upper layer are mixed with the warmer bottom layers.

The complexities of the hydrodynamic and thermal processes in a reservoir require the use of numerical models to provide an accurate description of the thermal and density stratification (Arai, 1973; Bonnet et al., 2000; Çalışkan and Elçi, 2009; Parker et al., 1975), as well as ice cover evolution (Imberger, 1982; MacKay et al., 2009). Water quality models of lakes and reservoirs can be formulated in different complexities ranging from a fully mixed zero-dimensional model to a complex three-dimensional one in space (Stefan et al., 1989). A large number of mathematical models have been developed over the years to model the water quality including temperature of reservoirs, most of which are one-dimensional models that consider variations in the vertical direction only. Some examples include CE-QUAL-R1(Environmental Laboratory, 1995), DYRESIM (Imerito, 2007), WESTEX (Fontane et al., 1993), WQRRS (USACE, 1986) and SELECT (Schneider et al., 2004). We also have some applications making use of two-dimensional models (with longitudinal and vertical elements), eg. CE-QUAL-W2 (Cole and Wells, 2008), BETTER (TVA, 1990); and three-dimensional computational fluid dynamics (CFD) models, eg. EFDC (Çalışkan and Elçi, 2009), FLOW-3D (Bender et al., 2007), and others. Higher order dimensional models (2D and 3D) require, in increasing order of complexity, detailed information on reservoir bathymetry and hydrological regimes including inflows and outflows, and boundary conditions (Martynov et al., 2012). Given the complexity in input data and the higher computational cost involved, one dimensional models are better suited for climate change impact studies of lakes and reservoirs that require multi-year simulations (Peeters et al., 2002). An important aspect of interest in cold regions is the evolution of the thermal regime during winter and its impact on the ice regime in the reservoirs themselves and the river reaches downstream of the reservoirs (Marcotte, 1980). To model these aspects, a reservoir hydrothermal model should also include in its formulation the formation, development and ablation of ice covers, so that the annual thermal cycle as well as the ice cover dynamics can be simulated.

There is growing consensus on human induced climate change (IPCC, 2007), and there has been considerable focus on assessing the impacts on socio-economic and bio-physical systems. The most commonly used tools to predict future climate conditions are global circulation models (GCMs). The GCMs are driven by greenhouse gas forcings corresponding to various possible paths of future development that lead to different emissions scenarios (Nakićenović and Swart, 2000). GCMs of the climate system suggest above global-average rates of future warming in the higher latitudes (Christensen, 2007). The GCMs have coarse spatial scales ($\geq$ 100km), though they have improved significantly over the years, and can fail to capture local variations in climate. For that reason, it has become a standard practice to use nested regional climate models (RCMs) driven by GCM forcing as boundary conditions. The RCMs have a higher spatial resolution (10 to 50 km) and are generally thought to be able to better capture local climatic variations. Warming of the climate system and other changes predicted by GCMs/RCMs will affect the water- and energy-balance of river systems in general and water reservoirs in particular. There have been a number of studies that have examined the potential impacts of future climate scenarios for lakes and reservoirs (Brown and Duguay, 2011; Dibike et al., 2011; Gebre et al., 2013; Sahoo and Schladow, 2008; Sahoo et al., 2011; Sahoo and Schladow, 2010). In northern regions, where there is a wider use of reservoirs for energy generation, navigation and as winter roads, the study of changes in the ice cover regime in the future is not only of scientific significance but also of societal interest, as changes in the ice cover regimes can have significant consequences for reservoir management.

The objective of this study is to examine the impact of climate change on the thermal characteristics and ice cover regimes of three regulated lakes (reservoirs) in Norway. We modify a one dimensional (1-D), process based lake thermal and ice cover model – *MyLake* (Saloranta and Andersen, 2007) to take into account the effect of reservoir outflows on the hydrodynamic and thermal regime of the reservoirs. The modified model is then used, after proper calibration and validation with observational data, for the climate change impact study. The three study sites: Follsjoe, Tesse and Alta, are selected based on data availability as well as to represent different hydro-climatic zones, namely, near coastal, inland and arctic, respectively. The main interest is to evaluate the changes in reservoir thermal structure, reservoir withdrawal temperatures and ice cover dynamics, i.e., duration and thickness. We make use of signals from two different GCMs that are dynamically downscaled with a RCM, and the changes are also investigated for two future time periods 2041-2070 and 2071-2100 compared to the baseline period that generally falls within 1981-2010. The results presented in this paper are not as such exact predictions due to the uncertainties inherent in the emissions scenarios, the climate models and the thermal and ice-cover model itself. However, they provide useful insight to the changes that might be expected under future climate scenarios.

2 STUDY AREA AND DATA

2.1 Study sites

The study was conducted on three reservoirs that are located in different climatic setting in Norway. The reservoirs are Follsjoe, Tesse, and Alta which are all regulated for hydroelectricity generation. Follsjoe is a near coastal reservoir and Tesse represents an inland/highland reservoir. Both of these reservoirs are sub-arctic. The Alta reservoir represents a northern reservoir in the arctic. The location of the three study sites is shown in

Fig. 1. Table 1 summarizes the physical characteristics of the three reservoirs that relate to the modeling work.

2.2 Data for model validation

The reservoir thermal balance and ice cover regime are determined by complex conditions of heat exchange with the atmosphere and the ground, as well as the hydraulic and morphometric peculiarities of the reservoir (Donchenko, 1966). Input data required for our modeling setup include: meteorological forcing to compute the energy balances on a daily time step, hydrological forcing data such as daily inflow and outflow discharges and inflow temperatures, and reservoir geometry. In addition, the model also requires observed vertical temperature profiles (multi-seasonal) as well as withdrawal temperature data for model validation. The required data sets were obtained from two data sources: all meteorological forcing data was obtained from the Norwegian Meteorological Institute (DNMI), while all other data pertaining to reservoir characteristics, hydrological data including observed water temperatures were obtained from the Norwegian Water Resources and Energy Directorate (NVE) data base.

Meteorological forcing: Meteorological input used to compute the energy balances include 2m air temperature (TM), precipitation (PR), 2m relative humidity (RH), 10m wind speed (WS), cloud cover (CC), air pressure (AP), and global radiation (GR). Air temperature and precipitation data are extracted from a 1x1km high resolution gridded data set from the Norwegian Meteorological Institute (Mohr and Tveito, 2008) by averaging over each of the reservoir areas. Data on the other meteorological variables with the exception of GR are obtained from nearby meteorological stations operated by Norwegian Meteorological Institute. Data on shortwave global radiation were not available and hence were estimated in the model using the Matlab Air-Sea Toolbox (Beardsley et al., 1998).

Hydrological forcing: The model requires daily inflow in m^3/day and inflow temperature data. The inflow was computed from the daily water balance of the reservoir using recorded daily reservoir volumes (or water surface elevations) and outflow discharges using the relationship: $I_t = V_t - V_{t-1} + O_t + E_t$ where I_t is the inflow (including direct precipitation on the reservoir), V_t and V_{t-1} are reservoir volumes at successive time steps O_t is the outflow (withdrawal + spill) and E_t is the evaporation. The evaporation is determined using the temperature based Thornthwaite method (Thornthwaite, 1948). We also need to specify the daily average withdrawal rates to compute the extent of the withdrawal layer as well as the heat advected due to the outflow discharges. Finally, we need measured vertical temperature profiles for model calibration/validation. In all the three reservoir sites, vertical temperature profiles at a single site close to the dams have been obtained from the NVE hydrological data base. In addition withdrawal temperatures data are obtained from the same data source and used for validation of withdrawal temperature simulations.

Reservoir geometry: We need to input the area distribution with depth, the outlet level(s), and the geometry of the reservoir cross section close to the outlet. The elevation-volume relationship was available for the reservoirs only up to the lowest regulated level. The modeling requires a full elevation-area relationship from the lowest point in the reservoir to the highest water level. We assumed a triangular volume-depth relationship to extend the curve to the bottom of the reservoir and hence derive a complete elevation area curve. Some level of errors will be introduced due to this assumption; however, it is believed that the errors will be quite insignificant in a one-dimensional model setup.

2.3 Scenario data

Meteorological forcing

The meteorological data corresponding to the Inter-Governmental Panel on Climate Change (IPCC) SRES A1B scenario (Nakićenović and Swart, 2000) were derived from two different GCMs: ECHAM5, developed by the Max Planck Institute for Meteorology, Germany (Roeckner et al., 2006) and HadCM3Q3 developed by the Hadley Centre, UK (Collins et al., 2011). The GCM outputs are dynamically downscaled to a 25km spatial resolution using the Rossby Centre Regional Climate Model RCA3 (Samuelsson et al., 2011) maintained by the Swedish Hydrological and Meteorological Institute, SMHI. The SRES A1B scenario is a medium-level emissions scenario that describes a technological emphasis leading to a balance across all sources of energy (Nakićenović and Swart, 2000). The RCA RCM downscaled data was obtained from the EU funded ENSEMBLES project for inter-comparison of RCMs (van der Linden P. and Mitchell, 2009) at the following webpage: http://ensemblesrt3.dmi.dk/.

Two widely used methods of transferring the climate change signals from RCMs to a model are the delta-change approach (Hay et al., 2000) and using the direct bias corrected Regional Climate Model (RCM) data, also called the direct or scaling approach (Teutschbein and Seibert, 2010). We use mainly the delta-change approach and make additional investigations using the direct method to gauge the uncertainty due to the bias correction approach The delta-change method is simple to implement and has been widely applied in climate impact research (Hay et al., 2000; Lawrence and Hisdal, 2011). The method essentially assumes that future model biases for both mean and variability will be the same as those in present-day simulations (Bader, 2008). Monthly delta-changes Δ_m, (in °C for temperature and in per cent for the five other elements) are derived as the difference between the mean monthly values for modelled 30 year future climate and the ones for the current climate (1981-2010). The daily values for the future climate for an element X are then computed as:

$$X_{i,m}(Future) = X_{i,m}(1981 - 2010) + \Delta_m \quad (1)$$

$$X_{i,m}(Future) = X_{i,m}(1981 - 2010) \times \left(1 + \frac{\Delta_m}{100}\right) \quad (2)$$

Where i is the day number and m is the month. Equation 1 is used for air temperature, and Equation 2 is used for the other five elements. In the direct or scaling approach, the mean monthly biases are computed by comparing the RCM derived data for the current period with observational data. The biases are then used to correct both the control and future scenario runs in a similar fashion as the delta-change method. Changes in the incoming global solar radiation (no-sky radiation) are not considered and changes in solar radiation reaching the air-water/ice/snow interface arise only as a result of changes in cloudiness.

For ease of presentation and discussion, we abbreviate the GCMs as Had (for HadCM3Q3) and Ech (for ECHAM5). We also name the four future scenarios based on the GCMs and future time periods as described below.

- Had4170 – HadCM3Q3 (2041-2070)
- Ech4170 – ECHAM5 (2041-2070)
- Had7100 – HadCM3Q3 (2071-2100)
- Ech7100 – ECHAM5 (2071-2100)

Figure 2 shows a comparison of the temperature changes (annual and winter) for the 2080s compared to the control period 1961-1990 for ensemble of 16 GCMs and three emissions scenarios (A2,A1B and B1) used in the IPCC 4th Assessment Report (IPCC, 2007) and the RCA RCM downscaled changes used in this study for the same period. The ensemble changes were generated using the web-based program at http://www.climatewizard.org/. The scenarios used in the present study generally represent close to median values (except the winter changes in Follsjoe and Tesse of Had7100 scenario). As lake thermal and ice cover regimes are mainly dependent on warming rates, the changes we reported could be regarded as medium level changes.

Future hydrological forcing

The use of a hydrological model is required to generate inflows for the future climate scenarios. We use the well-known HBV conceptual rainfall run-off model (Bergström, 1976) to derive expected changes in future inflow. The model simulates daily discharges using daily precipitation and temperature, and monthly estimates of potential evapotranspiration as input. There are a number of versions of the HBV model and the one used in this study is the *HBV-Light* Version 3 (Seibert, 2005). The model is semi-distributed where snow and soil moisture routines are computed for each of the ten elevation zones whereas the catchment response routine is lumped. Follsjoe and Tesse reservoir catchments have inter-basin water transfers and the HBV model was setup on nearby catchments to derive mean monthly changes (as a difference between simulated future and simulated current periods) in runoff in mm/day. These changes are then transferred to the respective reservoirs. For the case of Alta reservoir, there are no inter-basin transfers and the model is as such applied on the reservoir catchment itself with observed flows being computed by the daily water balance outlined earlier. Split-samples are used whereby half of the data is used for model calibration, and the remaining half for verification. For estimating inflow temperatures, a prediction model for inflow temperatures proposed by (Bartholow, 1989) is used. This equation is presented as Eq.3, and it has been successfully used to generate tributary inflow temperatures (Johnson et al., 2004).

$$T_i = A_0 + A_1 T_{aj} + A_2 \ln(Q_j) + A_3 \sin\left(\frac{2\pi j}{365}\right) + A_4 \cos\left(\frac{2\pi j}{365}\right) \quad (3)$$

where A_0 to A_4 are model parameters to be estimated from observed water temperatures, j is the day of the year from 1 to 365, Q_j is daily stream discharge. The model parameters are estimated using observational data for the respective reservoirs employing the “solver” function in Excel by minimizing the root mean squared error (RMSE) between observed and estimated water temperatures. Reservoir withdrawal discharges were derived using the nMag computer program for hydropower and reservoir operation simulation (Killingtveit and Sæalthun, 1995). The reservoir elevation guide curve was derived from long-term operation data and the same was used as input for deriving future production discharges.

3 MODEL SETUP

3.1 The thermal model

The change in temperature in a reservoir over time is a function of heat transfer due to internal mixing, vertical advection, atmospheric exchange at the air water interface, inflow and outflow (Fontane et al., 1981). A one-dimensional (1D) reservoir thermal simulation model has been used in this study. A 1D model assumes that the principal variation of flow characteristics (in our case water temperature) is in the vertical direction (Parker et al., 1975), and hence lateral variations are assumed negligible. The model used in this study is a modified version of the one dimensional lake thermodynamic model *MyLake* (Saloranta and Andersen, 2007; Saloranta et al., 2009), and we refer to the modified version in this paper as *MyLakeR* (where R denotes a reservoir). In its original version the model simulates thermal profiles and ice cover growth and ablation for lakes which have no through flows. We modified the model to take account of the water balance and advective heat transfers due to the outflows. In the model, the reservoir/lake is represented by horizontal layers of thicknesses Δz and horizontal areas $A(z)$, each of which is assumed to be fully mixed. The model then numerically solves the distribution of thermal energy, ice cover formation and ablation using the conservation of thermal energy for each vertical layer and an ice cover formation and decay algorithm which will be described later.

The general conservation of energy equation for any horizontal layer consists of diffusion, advection and a net heat source/sink term. In equation form it may be written as:

$$A\frac{\partial T}{\partial t} = \frac{\partial}{\partial z}\left[K_z A\frac{\partial T}{\partial z}\right] - A\frac{\partial (wT)}{\partial z} + A\frac{H^*}{\rho_w C_p} \qquad \textbf{(4)}$$

Where T is laterally averaged temperature (°C), z is space coordinate in the vertical direction (m), A is surface area of a particular element normal to direction of flow (m^2), K_z is vertical diffusion coefficient (m^2 day^{-1}), ρ_w is density of water (kg m^{-3}). H* (J d^{-1} m^{-2}) is the net heat flux for the given layer. C_p is the specific heat of water (kg °C J^{-1}), and w is the vertical advective velocity in a given layer (m day^{-1}). The second term to the right of Eq. 4 is what has been incorporated into *MyLakeR* to enable computation of advective heat transfer due to withdrawals in addition to diffusive and convective mixing.

Figure 3 illustrates the heat fluxes in a lake/reservoir during the open water and ice covered periods. The net heat flux H* at the air-water interface is given by:

$$H^* = H_{SW} + H_{LW} + H_{Sen} + H_{Lat} + H_{Sed} \qquad \textbf{(5)}$$

Where H_{SW} is the net solar radiation absorbed by the layer, H_{LW} is the net long-wave radiation, H_{Sen} and H_{Lat} are the net sensible and latent heat fluxes, and H_{Sed} is the heat flux at sediment-water interface (all in J m^{-2} d^{-1}). For the subsurface layers, only H_{SW} and H_{Sed} contribute to the local heating rate H^*. During the ice cover period only the sediment water flux and the shortwave radiations penetrating through snow and ice contribute to the local heating. Figure 3 shows the heat flux components during the open water and ice covered periods.

In order to compute all these fluxes the following daily meteorological variables should be provided as input series: air temperature at 2m height (°C), cloud cover (0-1), relative humidity (%), global solar radiation (J m^{-2} d^{-1}), wind speed at 10m height (m s^{-1}), air pressure at station level (hPa) and precipitation (mm d^{-1}). If solar insolation observations are not available (as is the case in our study), *MyLake* computes the global solar radiation (H_G) using Reed's bulk formula (Reed, 1977) as:

$$H_G = H_o\, \phi(\alpha) f(C)$$

$$\phi(\alpha) = 0.377 + 0.00513\alpha \qquad \textbf{(6)}$$

$$\begin{aligned} &f(C) = 1.0 - 0.62C + 0.0019\alpha \quad for\ C \geq 0.3, \\ &f(C) = 1 \quad for\ C < 0.3 \end{aligned}$$

Where C is the total cloudiness in tenth, α is noon (maximum) solar altitude in degree, and H_o is the downward extra-terrestrial (i.e., no-sky) solar radiation computed as a function of day of the year and geographical position using the MATLAB Air-Sea Toolbox (Beardsley et al., 1998).

The transmission and absorption of solar radiation in the snow, ice and within the water body are described by the Lambert-Beer law as $H_{SW}(z, t) = H_G(t)(1-\beta)\exp(-\lambda z)$, where $H_{SW}(z, t)$ is the net irradiance at depth z, H_G is the global incoming radiation, both in Jules, β is the albedo, and λ is the attenuation/extinction coefficient (m^{-1}). The albedo of water surface is computed from the atmospheric transmittance and sun altitude according to Payne (1972) using the Air-Sea Toolbox. Snow and ice albedos are input as parameters. During the ice covered period, solar radiation penetrating the snow-ice layer is attenuated according to $H_{SW}(z, t) = H_G(t)(1-\beta)\exp(-\lambda_i h_i)*\exp(\lambda_s h_s)$, where λ_i, λ_s are attenuation coefficients of ice and snow, h_i, h_s are ice and snow thicknesses, and β is the albedo of snow if $h_s > 0$ or albedo of ice if snow is not present.

MyLake also has a module to handle the heat exchange between water and sediments (H_{sed}). In our modelling setup, this has been disabled (for reducing simulation time) as model results were very insensitive to its inclusion. Hence, only heat exchange across the air-water interface was considered in the reservoir model *MyLakeR*. This simplification is reasonable for reservoirs of moderate depth considered in this study as the bottom area to volume ratio is relatively small (USACE, 1986; Wetzel, 2001a). The heat exchange between water and ice, H_{Wi} (Jm^{-2}) is computed as, $H_{Wi} = \left(T_{z,1} - T_f\right) C_w dz$ where $T_{z,1}$ is water temperature of the first layer, T_f is temperature of the under-layer of ice, C_w is the volumetric heat capacity of water (4.18e+6 J K^{-1} m^{-3}), and dz (=1m) is the layer depth (m).

3.2 Inflow placement and outflow dynamics

When a river enters a lake or reservoir, the incoming water will flow into a density layer that is most similar to its own density (Parker et al., 1975; Wetzel, 2001b). In *MyLakeR*, if the inflow density is less than that of the reservoir surface waters, the inflow water spreads over the reservoir surface. However, if the inflow density is higher than the temperature of the surface layer, the stream will plunge below the surface of the reservoir and placed on top of a layer which has higher density than the inflowing water.

During the simulation, the outflow discharge is predetermined and are given as input as daily average values. The withdrawal thickness (the layer in the reservoir that contributes to the flow) has to be determined to compute the withdrawal temperatures and the extent of advective mixing. The computation of the withdrawal temperature is illustrated for the case of a single outlet reservoir that is schematically represented in Fig. 4. The withdrawal layer that forms at the level of the outlet had been a subject of mathematical and experimental investigation for long (Imberger and Fischer, 1970; Imberger et al., 1976). For an idealized 2D situation (Steen and Stigebrandt, 1980), where the selective withdrawal approximates a line sink, the withdrawal thickness, δ, is given by $\delta = k1\sqrt{q/N}$ where q is the volumetric discharge per unit width (m^3/s/m) which is computed by dividing the volumetric discharge, Q, by the width of the reservoir, W at the outlet level. $N = \sqrt{-(g/\rho)(d\rho/dz)}$, is the Brunt–Väisälä buoyancy frequency which is a measure of the stability/strength of the density stratification. Reported experimental values include k1= 2.7±0.2 (Brooks and Koh, 1969) , and k1= 3 to 5 (Steen and Stigebrandt, 1980). We determine the values of k1 for each reservoir using a calibration procedure within the limits of the reported range of values.

Horizontal and vertical velocities in the withdrawal zone are determined using a method proposed by (Hocking et al., 1988). The method takes into account both the horizontal velocity variation in the vertical and the vertical motion of water falling (advection term) as water below it is withdrawn. The method used also assumes that the withdrawal layer, δ, is divided equally above and below the centre line of the outlet, although in general this may not be true. In the situation when the top half of the withdrawal thickness exceeds the water surface, the water surface elevation acts as the top limit of the withdrawal layer. In the same manner, if the bottom half of the withdrawal thickness exceeds the reservoir bottom, then the reservoir bottom acts as the lower limit of the withdrawal zone. If the withdrawal zone is beyond both the reservoir limits, then the whole water column gets mixed. The horizontal velocity distribution in the withdrawal layer is computed as (Hocking et al., 1988) :

$$u = \frac{1}{2}u_0\left(1 - \frac{x}{L}\right)\left[1 + \cos\pi\frac{z - z_s}{\delta_{1/2}}\right];\ 0 < \left|\frac{z - z_s}{\delta_{1/2}}\right| \qquad \textbf{(7)}$$

where L = the length of the fluid domain, in this case the reservoir, x is the horizontal distance from the outlet at which velocities and temperature profiles are computed (usually 300 to 400m away), and u_o is the maximum center line velocity. The total discharge Q can be found by integrating the velocity term over the withdrawal thickness, i.e.,

$Q(x,t) = B\int_{z_s-\delta_{1/2}}^{z_s+\delta_{1/2}} u(x,z)dz$ where B = the width of the reservoir. At the sink itself, $Q(0,t) = u_0 B\delta_{1/2}$ so that $u_0 = Q/B\delta_{1/2}$.

As water is withdrawn, water from above must fall to replace it. To compute the rate of fall or, in other words the vertical advective velocities, Hocking et al., (1988) integrated the two dimensional conservation of volume equation $\partial u/\partial x + \partial w/\partial z = 0$ to derive the vertical advective velocities as (z is positive in the downward direction) :

$$
\begin{aligned}
& w = u_o \frac{\delta_{1/2}}{L}; \qquad z - z_s \geq \delta_{1/2} \\
& w = u_o \frac{\delta_{1/2}}{2L}\left[1 + \frac{z - z_s}{\delta_{1/2}} + \frac{1}{\pi}\sin\pi\frac{z - z_s}{\delta_{1/2}}\right]; \qquad 0 \leq \left|\frac{z - z_s}{\delta_{1/2}}\right| < 1 \\
& w = 0; \qquad z - z_s < -\delta_{1/2}
\end{aligned} \tag{8}
$$

The advective velocity is constant until the water falls within the vertical bounds of the withdrawal layer, and the water below the withdrawal layer remains stagnant. Since $\delta_{1/2} \ll L$, the vertical velocity is much smaller than the horizontal velocity except near the top of the withdrawal layer and above.

The volume removed from each layer in the withdrawal zone, is calculated by multiplying the reservoir width by the velocity profile and the vertical grid step *dz*. The sum of all these volumes is calculated and compared to the observed one. A correction factor is applied so that these two volumes are equal to each other. Then, the temperature of the withdrawal water is calculated by using $T_w = \sum T_i V_i / V_{tot}$ where T_i = temperature of layer *i*, V_i =volume removed from layer *i*, V_{tot} = total withdrawal volume.

3.3 Mixing in the reservoirs

The two major factors that govern mixing in reservoirs are gravity and turbulence (EPA, 1969). Some level of mixing, though not significant compared to the above two, takes place by molecular diffusion. Gravity mixing (also called natural convection) occurs as a result of reservoir instabilities when upper layers of a reservoir become denser (due to warming or cooling) than lower layers. Turbulent mixing, on the other hand, occurs as a result of external energy sources that are classified into across the reservoir surface (due to wind), those advected in by inflows and energy introduced by the withdrawals (Fischer et al., 1979).

In the surface layers of reservoirs, wind causes an increase in the diffusive mixing and thereby the vertical diffusion coefficient. Such wind-induced diffusive action which takes place only during the ice-free period is accounted for separately in the model by the wind-mixing algorithm (Saloranta and Andersen, 2007). The total kinetic energy TKE (J) accumulated over one time step of 24 hours**,** available for wind-induced mixing is calculated by $TKE = W_{str} A_s \sqrt{\tau^3 / \rho_o}\, \Delta t$, where τ is wind stress ($N.m^{-2}$) calculated from the input wind speed data using the MATLAB Air-Sea Toolbox, A_s is the lake surface area, ρ_o is the density of the surface layer of water, W_{str} is a wind sheltering coefficient (between 0 and 1) which is calibrated during the modeling procedure.

Further, reservoirs will have increased mixing due to the vertical advection that could be generated because of velocity gradients as a result of inflow/outflow discharges (Fischer et al., 1979; Marcotte, 1980). In this study, the heat advected by the inflow is taken into account by adjusting the vertical diffusion coefficient K_z, whereas the heat advection due to the outflow is explicitly considered as shown in Eq. 1.

3.4 Ice-cover growth and decay

The model triggers ice formation when water layer temperature drops below the freezing point and the temperature of the super-cooled layers is set to the water freezing point. The sensible heat deficit in the super-cooled layer is turned into a latent heat of freezing and an initial ice-layer defined as frazil ice is created. Before the formation of an ice-cover, ice-crystals are suspended in the water column and grow until they float to the surface and form a slushy layer which freezes to form the initial ice-cover. The thickness of frazil ice increases whenever new super-cooled water is encountered, and decreases whenever the water column receives heat to melt the frazil ice. The initial solid ice-cover, associated to the freeze-up date predicted by the model, only appears when the accumulation of frazil ice reaches a threshold thickness of 3 cm (Saloranta and Andersen, 2007). Once a solid ice cover has been formed, the growth of ice thickness takes place from the bottom (congelation ice) or from the top (snow ice). The additional ice thickness due to congelation ice growth is calculated whenever the air temperature T_a (°C) is below the freezing point using Stefan's law (Leppäranta, 1993).

$$h_{ice\_new} = \sqrt{h_{ice}^2 + \frac{2\kappa_{ice}}{\rho_{ice} L}(T_f - T_{ice})\Delta t} \qquad \textbf{(9)}$$

where κ_{ice} (W. °C^{-1}.m^{-1}) is the thermal conductivity of ice, ρ_{ice} (kg.m^{-3}) the density of ice, L (J.kg^{-1}) the latent heat of freezing, Δt (s) the daily time step. Snow ice formation occurs when the weight of snow cover exceeds the buoyancy capacity of the ice layer, the ice surface submerges and water floods on the top of ice (Bengtsson, 2012; Dibike et al., 2011). This water mixes with the lower layer of the snow cover and forms a slush and becomes snow ice (also called white ice) when it freezes. The thickness of a new snow-ice is computed in the model as:

$$\Delta h_{si} = \max\left[0, h_{ice}\left(\left(\frac{\rho_{ice}}{\rho_w}\right)-1\right)+h_{s\_weq}\right] \tag{10}$$

Where h_{s_weq} is the thickness of the snow layer in water equivalents. White-ice properties are assumed to be the same as congelation ice, and the newly formed white-ice layer is subtracted from the snow cover and added to the ice layer.

Lake ice decay or melt is computed by considering the net heat flux at the air-snow or air-ice interface. The net heat flux is used to melt the snow cover first before ice melt starts. The formulation for melt (snow and ice) is given as:

$$melt_{i,s} = \max\left[0, \frac{\left(1-A_{coeff}\right)*H_{SW}+H_{LW}+H_{SL}}{\rho_{i,s}*L_{i,s}}\right] \tag{11}$$

Where i and s refer to snow and ice, A_{coeff} is the ice/snow attenuation coefficient, H_{SW} is the net short wave radiation, H_{LW} is the net long wave radiation, H_{SL} is the net sensible and latent heat flux, $\rho_{i,s}$ is the density of ice/snow and $L_{i,s}$ is the latent heat of ice/snow.

3.5 Numerical approximation and calibration procedure

The numerical approximation used in *MyLakeR* for solving Eq. 1 is a hybrid exponential difference scheme (Saloranta and Andersen, 2007) based on (Dhamotharan et al., 1981). This solution scheme is stable as errors of the difference scheme from the true solution of the differential equation are not the result of propagation of numerical errors (Environmental Laboratory, 1995).

Model parameters and coefficients usually show wide ranges for different applications. In this study, initial estimates were done from literature values. A total of nine model parameters have been included in the optimization routine: diffusion coefficient during ice free period, diffusion coefficient during ice covered period, wind sheltering coefficient, snow albedo, ice albedo, attenuation coefficients for water, snow, and ice; and the coefficient defining the withdrawal thickness (k1). An automatic optimization routine has been integrated to the *MyLakeR* code so that model parameters can be varied within the literature ranges automatically and optimized. The objective function is minimizing the root mean squared error (RMSE) between computed and observed vertical temperature profiles. All available data set has been used and all observation points (summer and winter for example) are given equal weights in the error computation. The optimization routine used is a constrained nonlinear optimization that uses the Nelder-Mead simplex algorithm (Nelder and Mead, 1965), which is one of the most widely used direct search methods.

4 RESULTS

4.1 Model calibration/validation

The meteorological and hydrological forcing data are provided at a daily time step. Figure 5 shows the climatology of forcing data in terms of mean monthly values over the simulation period. Similarly, Figure 6 shows the hydrological forcing summary: reservoir inflow, inflow temperature, reservoir outflow and outflow temperatures for each of the three reservoirs as mean monthly values. The baseline period that is also used for model validation is 1988-2006 for Alta, 1988-2008 for Follsjoe, and 1984-2008 for Tesse.

Water temperature profiles and withdrawal temperatures

Simulations were started with the first available vertical temperature profile measurement in the ice free period and continued until late 2000s. The water temperature values are determined daily for every horizontal slice that is 1m thick. The model was calibrated and validated by adjusting model parameters within reported ranges in literature. The parameter adjustment was made using an automatic optimisation routine that has its objective function to minimise the root-mean-squared errors between observed and simulated vertical temperature profiles. All of the model simulations for the current and future climate scenario comparisons were then made using the calibrated model parameters. In addition, the same boundary conditions in terms of initial temperature profiles were considered for the scenario simulations. Table 2 shows the calibrated model parameters for each of the three reservoirs. The observations used for the validation (calibration and verification) of vertical temperature profiles include 685 point measurements for Follsjoe, 924 for Tesse and 2694 for Alta.

Alta is quite a very small reservoir compared to the inflow. The reservoir storage capacity is just 6% of yearly inflow to the reservoir (Asvall, 2007). The flow through the reservoir is too fast (i.e. having low residence time), and hence there is not adequate time for strong stratification to develop as turbulent mixing is too rigorous (Fischer et al., 1979). This reservoir was validated reasonable well by considering a very high value of diffusive mixing well above the normal range for storage reservoirs or lakes.

When a reservoir is ice covered, the thermal stratification is very weak, and there is little vertical transmission of heat by convective mixing; and there is no mixing due to wind action (Bengtsson, 2012). The mixing mechanisms that dominate are hence the vertical diffusion and advection. Due to large withdrawal rates in winter, the advective mixing was the dominant mode of mixing. Wind speeds over lakes/reservoirs are significantly higher than over land due to less friction over the water surface (Schmidlin, 2005). As our wind speed data come from land based stations, it is most likely that the wind mixing is underestimated, and hence the model compensates for this by increasing the diffusivity coefficient. To get the heat balances reasonably close in winter, we had to reduce the advective mixing during the ice covered period by a factor of 0.65 in Follsjoe reservoir, and 0.10 in both Tesse and Alta reservoirs.

These reductions can be physically explained partly by the higher diffusivity coefficients used to compensate for wind mixing underestimation during the open water period, and partly by reservoir morphometry related effects.

To confirm the robustness of model parameters, the goodness-of-fit statistics were computed by dividing the period of observations into two equal periods (named calibration and verification as shown in Tables 3 and 4. The performances of the two periods are then compared with the overall performance. It has been observed that the model performed more or less equally well between the periods, proving the robustness of the temperature validation. Calculation of goodness-of-fit statistics for the comparison of modelled and measured temperature profiles (using all measurement points) produced mean bias errors (MBE) of +0.33, +0.11 and +0.02 ºC, for Alta, Follsjoe and Tesse respectively. The mean absolute errors (MAE) were 0.68 ºC, 0.61 ºC and 0.60 ºC, in the same order. The Nash-Sutcliffe (NS) efficiency values were all $\geq$ 0.90. The results indicate that the model reasonably captured the energy budget and thermal characteristics of the reservoirs and thus can be used to assess the impacts of a changed climate in the future. The validation of the current climate simulation against observed vertical water temperature profiles as well as withdrawal temperatures are shown in Fig. 7 and Fig. 8, respectively. The RMSE for observed vertical temperature profiles is less than 1 ^{o}C whereas that for withdrawal temperatures is less than 1.5 ^{o}C.

Ice phenology, ice thickness and snow depth

In addition to water temperature profiles, important aspects of model validation are the correct representation of ice phenology and thickness. However, only Tesse has got both ice phenology and ice thickness observations. In addition, we have also data on snow thicknesses. Follsjoe has no ice and snow related observations, whereas for Alta we have got only ice and snow thickness observations. For the case of Tesse freeze-up is simulated with a mean bias error MBE (bias) of -4.6 days (earlier than the observed) and a mean absolute error MAE of +7.0 days. On the other hand, break-up is simulated with a MBE of +0.7 days later and a MAE of +6.8 days. Overall the model is able to reasonably hindcast the observed ice phenology for this reservoir. We compared 89 measurements of snow cover and total ice thickness over the period 1987 to 2008, with that simulated by the model and we found that total ice thickness is simulated with a MBE of -0.13 cm and a MAE of 7.9 cm whereas snow cover thicknesses were simulated with a MBE of 7.9 cm and a MAE of 9.7 cm. The correlation coefficient between observed and simulated total ice thickness was 0.78. For the case of Alta Reservoir we have only 35 measurements of ice and snow thicknesses between the years 1998 and 2008. The comparison shows that total ice thickness was simulated with a MBE = -5.7 cm and MAE = 9.8 cm, whereas snow depth over ice was simulated with a MBE = -2.2 cm and a MAE = 5.5 cm. The comparisons are graphically illustrated in Fig. 9. Overall, the errors in ice phenology and ice thickness are within the margins or less than previously reported values for lake ice thickness simulation using 1D models (Brown and Duguay, 2011; Dibike et al., 2011), indicating that MyLake has produced satisfactory simulations for the two reservoirs.

4.2 Model forcings for future climate

Meteorological forcing

Monthly change signals in all six meteorological input forcings are derived from dynamically downscaled RCM data with a 25km resolution for the two future time periods and two GCMs used in the study. Figure 10 shows for each month the monthly change signals for each of the two future periods and the two dynamically downscaled GCM outputs. In general, the future scenarios depict a warmer climate with winter warming higher than the rest of the season. In addition, we generally see a wetter future period with precipitation increases more or less distributed uniformly across the seasons. The scenarios also depict an overall reduction in wind speed by up to ~ 10 % though decreases by up to ~ 10 % are also projected in a few cases. Changes in relative humidity are within ~ ± 6% whereas changes in cloud cover vary in the range of ~ ± 10%. Air pressure changes are relatively insignificant with changes falling in the range of ~ ± 0.5%. The daily values in future forcings are then obtained by applying the change signals to the observational data.

Hydrological forcing

Flow regime alterations as a result of changes in meteorological forcing due to climate change were determined using a calibrated HBV model (*HBV light*). The hind-casted inflows for Follsjoe and Tesse that we used in the baseline simulation comprise diversions from nearby catchments, and an upstream regulated reservoir in case of Follsjoe. For this reason, we used a nearby natural catchment called Søya (catchment area ~150 km^2) for computing inflow changes for Follsjø and nearby catchment Sælatunga (catchment area ~ 460 km^2) for computing inflow changes to Tesse. The Alta catchment (catchment area = 5940 km^2) has neither diverted flows nor upstream regulations, and hence the catchment itself has been calibrated at the dam site with the inflows computed using the daily water balance.

The NSE for calibration and validation are shown in Table 5 which shows reasonably good model performance. The calibrated models were then driven with the future scenario forcing to obtain the changes in inflow. The changes derived from model simulations for the current and future scenarios are then used to derive future inflows for the three reservoirs. Two significant changes were observed in the hydrological regimes at all three reservoir sites: 1) large increases in winter flows, 2) reduction of late spring and summer flows, as shown in Fig. 11. This is in line with IPCC report (Kundzewicz, 2007) which states that peak streamflow is likely to move from spring to winter in many areas due to early snowmelt, with lower flows in summer and autumn. Overall, HadCM3Q3 forcing gives an increase in the annual inflow at all three reservoir sites in the range of 0 % to 38 %, whereas ECHAM5 gives an increase (24% to 35%) in Alta and a decrease between -1% to -12% in the case of Tesse and Follsjoe. The inflow temperatures for the future scenarios were derived from Bartholow's formula (described in the methods section) with parameters calibrated during the observation period. The calibration resulted in a good fit with RMSE and coefficient of determination, R^2 of Follsjoe (0.29 ºC, 1.00), Tesse (0.52 ºC, 0.99), and Alta (0.35 ºC, 1.00).

We derived reservoir withdrawal discharges using the nMag computer program for hydropower and reservoir operation simulation (Killingtveit and Sæalthun, 1995). The reservoir elevation guide curves were derived from long-term operational data and the same was used as input for deriving future production discharges.

4.3 Climate change impacts

We present the results of the model predictions for possible future conditions under climate change focussing mainly on the ice and snow cover regime, and the thermal regime. Our main interest is to look at mean changes in the ice cover and snow regimes (freeze-up date, break-up date, ice cover duration, ice thickness, and snow thickness) and temperature regimes (withdrawal temperatures, surface temperatures and bottom temperatures).

Ice cover and snow in the future climate

The ice cover regime is characterized by the ice phenology (freeze-up, break-up, and ice cover duration) and ice thickness (maximum annual and time distribution). The results showed (see Table 6) a later freeze-up by 6 - 9 days (Alta), 20 - 27 days (Follsjoe), and 9 - 11 days (Tesse) by the 2050s. By the 2080s, on the other hand, freeze-up is delayed by 11-14 days (Alta), 42 days (Follsjoe) and 16-18 days (Tesse). Break-up dates are advanced by 6-10 days (Alta), 30-31 days (Follsjoe), and 7-12 days (Tesse) by the 2050s. By the 2080s the advance in break-up dates ranges from 14-16 days (Alta), 38-47 days (Follsjoe), and 13-18 days (Tesse). Overall, ice cover duration will be reduced by 15-16 days (Alta), 50-58 days (Follsjoe) and 18-21 days (Tesse) by the 2050s. The corresponding reduction in ice cover duration by the 2080s will be 27-28 days (Alta), 80-89 days (Follsjoe) and 29-36 days (Tesse). Though there are slight inter-GCM differences, the results show that the near-coastal reservoir Follsjoe will have its ice cover duration reduced almost three times as much as the other two reservoirs. The number of ice free winters in Follsjoe Reservoir will increase from 0/19 (0 out of 19 winters) during the baseline period to 1/19 in the 2050s (both scenarios) and 3/19 in the 2080s (both scenarios). The inland Tesse and arctic Alta reservoirs will not have any ice free winters either in the 2050s or 2080s.

Inter-annual variability in ice phenology as measured by the standard deviation (SD) also showed significant changes in the future climate for Follsjoe Reservoir. The SD in the comparisons below has been rounded to the nearest full days. SD for freeze-up varied from 18 days in the baseline period to 26-29 (2050s) and 30 days (2080s), while for break-up it varied from 9 days in the baseline period to 25-31 days (2050s) and 16-17 days (2080s). Tesse showed only slight increases in inter-annual variability in the future climate: freeze-up variability will increase from 10 days for the baseline to 14 days (2050s) and 15-25 (2080s), break-up variability will increase from 6 days for the baseline to >6-7 days (2050s) and 8-13 days (2080s). Alta in the arctic depicted even lesser increase in future variability: freeze-up from 6 days in the baseline to 6-8 days in both the 2050s and 2080s. The variability in break-up showed no change in the 2050s (baseline =4 days) and increased to >4 -5 days in the 2080s.

The dominant climatic variables that influence ice cover dynamics are the air temperature and the snow conditions (Brown and Duguay, 2011). The snow cover conditions are in turn very much dependent on the air temperature, as air temperature determines whether precipitation falls as rain or snow. With the greater warming in winter projected by the GCMs, there will be a significant reduction in the freezing degree days. In addition, part of the precipitation that comes as snow in the present climate will change its form to rainfall thereby influencing snow depths and ice growth. The scenario application showed that maximum snow depths will be reduced in the three reservoirs (Alta: 3-5 cm (2050s), 5-9 cm (2080s); Follsjoe: 7-8 cm (2050s), 10-11cm (2080s); Tesse: 3-6 cm (2050s), 5-8 cm (2080s)). The change in ice thickness i.e., reduction is of a much larger magnitude (Alta: 5-13 cm (2050s), 16-22 cm (2080s); Follsjoe: 34-36 cm (2050s), 38-47 cm (2080s); Tesse: 7-12 cm (2050s), 13-18 cm (2080s)). As with the ice phenology, the near-coastal Follsjoe showed much larger order of magnitude of ice thickness reductions compared to the other two reservoirs. Table 6 summarizes the projected changes in ice phenology, maximum annual ice thickness and maximum annual snow depth for the four scenarios. Figure 12 depicts the mean annual ice thickness and snow depth progression for the baseline and the four scenarios.

Changes in thermal regime

We investigated changes in withdrawal temperatures as well as the duration of thermal stratification. For analysing the pattern of stratification, the onset of stratification is defined as the date at which the surface to bottom temperature difference is above 3 ^{o}C , and end of stratification is defined as the first day of isothermal temperature after the onset of stratification (Blenckner et al., 2002) based on (Fang and Stefan, 1999). Surface and bottom temperatures are taken respectively as the mean temperature of the top and bottom 1m thick layers. Figure 13 shows the withdrawal temperatures under the baseline and the four future scenarios. All reservoirs show an increase in temperature during the ice free period. The changes in the ice covered period are very marginal. Withdrawal temperatures are computed assuming a more or less similar operation regime of the reservoirs as in the current period.

This assumption may not hold in the future as power utilities will adjust their operation regime in the future to accommodate the changed inflow regime as well as possible changes in demand regimes. Hence, the results are only indicative values.

The ice-off dates will advance in the future scenarios compared to the base period by between 6 to 14 days in the arctic Alta, 7 to 18 days in the inland Tesse and by a larger margin of 30 to 47 days in the near coastal Follsjoe (Table 6). This implies that the thermal stratification will begin significantly earlier than is observed under the baseline climate. Alta reservoir is never stratified in the current as well as future scenarios (maximum temperature difference for the baseline being 2.2 ^oC and scenarios between 2.2 and 2.4 ^oC). Hence, discussions of changes in thermal stratification will be limited to Follsjoe and Tesse reservoirs. For Follsjoe the baseline difference is 8.2 ^oC whereas the four scenarios range in between 7 (Had4170) to 8 ^oC (Ech4170). The onset of summer stratification is advanced by 6 days for Ech4170, 9 days for Had4170, and 11 days for both Had7100 and Ech7100. At the same time, the end of stratification is delayed by 11days (Had4170 and Had7100), and 25 days (Ech4170 and Ech7100). For the case of Tesse Reservoir, the maximum difference between surface and bottom temperature is 5.5 ^oC for the baseline and between 5.5 (Had4170) and 7.1 ^oC (Ech7100) for the scenarios. The onset of thermal stratification is advanced by 10 days (Had4170 and Ech4170) and 18 to 20 days (Had7100 and Ech7100). On the other hand, the end of stratification is delayed by 11 days (Had4170 and Ech4170) and 16 to 18 days (Had7100 and Ech7100).

Sensitivity of future changes to meteorological and hydrological forcing

In order to gauge the relative importance of direct meteorological forcing influencing the heat fluxes at the air-water or air-snow/ice interface versus the indirect hydrological forcing, we carried out simulations using the scenario meteorological forcing keeping the hydrological forcing the same as in the base line scenario. We considered the two end-of-century scenarios (Had7100 and Ech7100) for this purpose, and simulations were carried out for the near coastal Follsjoe Reservoir which has shown higher sensitivity to climate change scenarios compared to the two other reservoirs. Figure 14 shows the comparison of ice phenology and ice thickness as well as withdrawal temperatures for the two end-of-century scenarios. The results show that hydrological forcings are especially significant for withdrawal temperature. On the other hand, ice phenology and ice thickness changes seem to be governed by meteorological forcing, with hydrological forcing having only a relatively marginal importance. Mean differences in freeze-up dates were only 3 for both scenarios days whereas it was between 2 and 3 days for break-up. The differences in computed mean maximum annual ice thicknesses were just 0.10 cm for Ech7100 and 0.2 cm for Had7100.

Sensitivity to method of bias correction

Meteorological data from RCMs are subject to biases, when the RCM output is compared with observations of the same time period. We have outlined in our methodology, two methods that are often used for bias correction, namely, the delta-change approach and the direct approach. The delta-change approach uses observed data as the baseline, and the observations are perturbed with monthly change signals, derived from RCM output for the current and future periods, to get data corresponding to the future period. In the direct method, however, the bias corrected RCM outputs (for the corresponding periods) are used as both the baseline and future data. The delta-change approach was the one selected in this study due to its simplicity and wider use in hydrological modeling studies. However, we carried out some sensitivity studies by applying the direct method to the Follsjoe reservoir and comparing the simulation results to the results we reported using the delta-change method of bias correction. The thermal and ice cover regime of reservoirs is mainly dependent on the net surface heat fluxes, the wind stress at the surface (Sahlberg, 2003) and the snow cover regime. We compared the net surface heat flux for Follsjoe computed based on the delta-change and the scaling approach. The net surface heat fluxes computed using observational meteorological data and the bias-corrected forcing from the two GCMs are reasonably close (Fig. 15a). The same applies to future datasets as shown in Fig. 15b. With regard to ice thickness and snow depths, the bias corrected data sets generally produce higher ice and snow thicknesses which can be explained, at least partly, by the difficulty to reasonably bias-correct precipitation data.

Comparison of the mean simulated ice and snow regimes using bias-corrected RCM control period data (direct method) (Table 7) to those simulated using observational data showed almost no differences for HadCM3Q3 forcing. The differences for ECHAM5 were very large for freeze-up (13 days) and break-up (19 days), although maximum ice and snow thicknesses were simulated reasonably close. The results suggest that the method of bias correction can produce significant differences in the expected magnitude of future changes depending on the GCM forcing being used for the study. One way to take account of the uncertainty in the bias-correction method is to apply both methods and take the average of the changes resulting from each of them. Based on this, freeze-up will be delayed 36 days (Had7100) and 35 days (Ech7100). Break-up, on the other hand, will be advanced 43 days (Had7100) and 44 days (Ech7100). The expected reductions in maximum annual ice thickness are also pretty much close, 43 cm (Had7100) and 44 cm (Ech7100); whereas maximum annual snow depths will be reduced by 11 cm (Had7100) and 10 cm (Ech7100).

5 DISCUSSION AND CONCLUSIONS

A multi-year lake thermodynamic model MyLake has been modified to take into account the hydrodynamics and advective mixing of reservoir through flows. The model was validated by applying it to three reservoir sites and fitting parameters to hindcast measured temperature profiles, withdrawal temperatures and ice and snow cover data. The model was well validated using continuous multi-year simulation for the three reservoirs. The vertical temperature profiles were predicted with an overall RMSE of 0.77 ^{o}C for Tesse 0.80 ^{o}C for Follsjoe and 1.13 ^{o}C for Alta Reservoir. The predictions of the withdrawal temperatures were also simulated well with a RMSE value of 1.02 ^{o}C for Follsjoe and 1.30 ^{o}C for Alta. Overall, the model was able to capture the thermal balance of the reservoirs and can make credible predictions of future conditions under changed meteorological and hydrological forcing.

We had limited ice cover data for model validation. There is no ice related data on the Follsjoe reservoir. Tesse has both ice phenology and ice and snow cover thickness data. Alta, on the other hand, has only measurements of ice and snow thicknesses. However, based on the limited validation, the model seems to have captured the ice formation dynamics pretty well though snow depths were poorly correlated.

Although inter-GCM variability exists, the results generally depict a marked reduction in ice cover duration (Fig.16a). In the near coastal Follsjoe Reservoir, the ice cover duration will be reduced by 44 to 53 days in 2050s, and by 57 to 81 days in 2080s. The inland-highland reservoir Tesse shows a reduction in ice cover duration by 18 to 21 days in 2050s and 29 to 36 days in 2080s. Alta Reservoir in the arctic will have its ice cover duration reduced by 15 to 16 days in 2050s and 27 to 28 days in 2080s. Generally, the two GCMs produced very similar changes for Alta and Tesse, whereas the inter-GCM variability in Follsjoe was much larger, especially in the 2080s. Maximum annual ice thickness changes (Fig. 16b) are also much higher for the Follsjoe (34 to 36 cm in 2050s, 43 to 45 cm in 2080s) compared to Tesse (9 to 18cm in 2050s and 17 to 29cm in 2080s), and Alta (5 to 13cm in 2050s and 16 to 22cm in 2080s).

There are multiple sources of uncertainty in climate change impact studies as the one we embarked on. These may be summarized as (Chen et al., 2011; Gardelin et al., 2003; Jones, 2000; Maurer, 2007): 1) the uncertainty in the forcing of the GCMs, i.e., in the emissions scenario, 2). the uncertainty due to different GCMs which give different outputs to the same forcing, 3) the uncertainty introduced by the downscaling of the coarse GCM results to finer resolution using the regional climate model, 4) the uncertainty introduced in the bias-correction procedure , and 5) uncertainty in the impact assessment models – hydrology and thermal model (model structure and parameter uncertainties). This study has made use of RCM simulations in the ENSEMBLES project (van der Linden P. and Mitchell, 2009) which has used the medium level A1B emissions scenario in the RCM inter-comparison. Hence, it was not possible to consider different emissions scenarios. However, from the comparison of multi-emissions scenarios using 16 GCMs that we showed in Fig. 2 the warming rates we considered correspond to near-median values. We have made use of two different GCMs and the uncertainty due to differences in GCMs is hence considered albeit using only two GCMs. The uncertainty due to RCMs can be addressed by making use of a multiple of RCMs and looking at the sensitivity of the model results, which has not been considered in this study due to resource limitations. We have accounted for the uncertainty in the bias-correction procedure by considering two different bias correction approaches (the delta-change and the direct approach). The results have shown to be less sensitive to the method of bias correction. Finally, this study has assumed model stationarity of the lake thermal model as well as hydrological model. Hence, model uncertainty has not been accounted for which is another limitation of this study. In general, it is difficult to quantify (using available methods) the importance of the different sources of uncertainty.

Overall, the case studies we presented in this paper provide some insight into the probable responses of reservoirs under future climate scenarios. The impacts of these changes on the water quality and biota in the reservoirs and the receiving rivers downstream are a matter of interest for future research. Our study has assumed that reservoir operation regimes in the future are similar to those at present, which may not hold true under changed hydrological conditions in a future climate. Hence, another line of future research could be investigating the synergistic effects of possible changes in operation regimes in a changed climate in the future.

Acknowledgments

This study was funded mainly by research grant to the first author from the Norwegian Research Council through the Sustainable Infrastructure Project (Project No. 81143700). We also acknowledge supplementary grants from the Centre for Environmental Design of Renewable Energy – CEDREN. Research cooperation with the Nordic Centre of Excellence, CRAICC is also acknowledged. We thank Tuomo Saloranta for providing the *MyLake* model code and additional assistance. We are grateful to Ånund Kvambekk at the Norwegian Water Resources and Energy Directorate for providing ice data. All other data sources mentioned in the "*Study Area and Data*" section are gratefully acknowledged.

References

Arai, T., 1973. Thermal structure of the artificial reservoir. In: G.F. White, E.B. Worthington and W.C. Ackermann (Editors), Man-made Lakes: Their Problems and Environmental Effects. Geophys. Monogr. Ser. AGU, Washington, DC, pp. 536-538.

Asvall, R.P., 2007. Selective withdrawal to reduce regulation effects on ice cover downstream outlet of Alta power plant 14^{th} Workshop on River Ice. CGU-HS Committee on River Ice Processes and the Environment, Québec, Canada, pp. 11.

Bader, D.C., C. Covey, W.J. Gutkowski, Jr., I.M. Held, K.E. Kunkel, R.L. Miller, R.T. Tokmakian, and M.H. Zhang, 2008. Climate Models: An Assessment of Strengths and Limitations. U.S. Climate Change Science Program Synthesis and Assessment Product 3.1, Department of Energy, Office of Biological and Environmental Research, pp. 124.

Bartholow, J.M., 1989. Stream temperature investigations: Field and analytic methods, Instream Flow Information Paper No. 13, Biological Report 89 (17). U.S. Fish and Wildlife Service, Grand Junction, Colo.

Baxter, R.M., 1977. Environmental effects of dams and impoundments. Annu. Rev. Ecol. Syst., 8: 255–283.

Beardsley, R.C., Dever, E.P., Lentz, S.J. and Dean, J.P., 1998. Surface heat flux variability over the northern California shelf. Journal of Geophysical Research: Oceans, 103(C10): 21553-21586.

Bender, M.D., Kubitschek, J.P. and Vermeyen, T.B., 2007. Temperature modeling of Folsom Lake, Lake Natoma, and the Lower American River Bureau of Reclamation,Technical Service Center Sacramento County, California, pp. 184.

Bengtsson, L., 2012. Ice covered lakes. In: R.W.H. L. Bengtsson, R.W. Fairbridge (Editor), Encyclopedia of Lakes and Reservoirs, pp. 357-360.

Bergström, S., 1976. Development and application of a conceptual runoff model for Scandinavian catchments, University of Lund, Lund, 134 pp.

Bevelhimer, M., Alavian, V., Miller, B. and Hauser, G., 1997. Modeling Thermal Effects of Operational and Structural Modifications at a Hydropower Facility on a Premier Trout Stream in Southwestern Montana, Waterpower ‘97: International Conference on Hydropower, Trondheim, Norway, pp. 40-49.

Blenckner, T., Omstedt, A. and Rummukainen, M., 2002. A Swedish case study of contemporary and possible future consequences of climate change on lake function. Aquatic Sciences, 64(2): 171-184.

Bonnet, M.-P., Poulin, M. and Devaux, J., 2000. Numerical modeling of thermal stratification in a lake reservoir. Methodology and case study. Aquatic Sciences, 62(2): 105–124.

Brooks, N.H. and Koh, R.C.Y., 1969. Selective withdrawal from density-stratified reservoirs. Journal of Hydraulics Div., ASCE, 95(HY4): 1369-1400.

Brown, L.C. and Duguay, C.R., 2011. The fate of lake ice in the North American Arctic. The Cryosphere, 5: 869-892

Çalışkan, A. and Elçi, Ş., 2009. Effects of Selective Withdrawal on Hydrodynamics of a Stratified Reservoir. Water Resources Management, 23(7): 1257-1273.

Chen, J., Brissette, F.P. and Leconte, R., 2011. Uncertainty of downscaling method in quantifying the impact of climate change on hydrology. Journal of Hydrology, 401(3–4): 190-202.

Christensen, J.H., B. Hewitson, A. Busuioc, A. Chen, X. Gao, I. Held, R. Jones, R.K. Kolli, W.-T. Kwon, R. Laprise, V. Magaña Rueda, L. Mearns, C.G. Menéndez, J. Räisänen, A. Rinke, A. Sarr and P. Whetton, 2007. Regional Climate Projections. In: S. Solomon et al. (Editors), Climate Change 2007: The Physical Science Basis. Contribution of Working Group I to the Fourth Assessment Report of the Intergovernmental Panel on Climate Change. Cambridge University Press, Cambridge, United Kingdom and New York, NY, USA.

Cole, T.M. and Wells, S.A., 2008. CE-QUAL-W2: A two-dimensional, laterally averaged, hydrodynamic and water quality model, version 3.1, Instruction Rep. EL-2002-1, U.S. Army Engineering and Research Development Center, Vicksburg, MS.

Collier, M., Webb, R.H. and Schmidt, J.C., 1996. Dams and rivers: A primer on the downstream effects of dams, U.S. Geological Survey, Denver, pp. 94.

Collins, M., Booth, B.B., Bhaskaran, B., Harris, G., Murphy, J., Sexton, D.H. and Webb, M., 2011. Climate model errors, feedbacks and forcings: a comparison of perturbed physics and multi-model ensembles. Climate Dynamics, 36(9-10): 1737-1766.

Dhamotharan, S., Gulliver, J.S. and Stefan, H.G., 1981. Unsteady one-dimensional settling of suspended sediment. Water Resources Research, 17(4): 1125-1132.

Dibike, Y., Prowse, T., Saloranta, T. and Ahmed, R., 2011. Response of Northern Hemisphere lake-ice cover and lake-water thermal structure patterns to a changing climate. Hydrological Processes, 25: 2942-2953.

Donchenko, R.V., 1966. Peculiarities of ice cover formation on reservoirs. In: L.J. Tison (Editor), Hydrology of Lakes and Reservoirs. International Association of Scientific Hydrology, pp. 564-574.

Environmental Laboratory, 1995. CE-QUAL-R1: A numerical one-dimensional model of reservoir water quality; User's manual, U.S. Army Engineer Waterways Experiment Station, Vicksburg, MS, pp. 519.

EPA, 1969. Mathemetical models for the prediction of thermal energy changes in impoundments, Water Quality Office, Environmental Protection Agency, Washington, D.C., pp. 157.

Fang, X. and Stefan, H.G., 1999. Projections of Climate Change Effects on Water Temperature Characteristics of Small Lakes in the Contiguous U.S. Climatic Change, 42(2): 377-412.

Fischer, H.B., List, E.J., Koh, R.C.Y., Imberger, J. and Brooks, N.H., 1979. Mixing in Reservoirs, Mixing in inland and coastal waters. Academic Press, New York, pp. 148-228.

Fontane, D.G., Howington, S.E., Schneider, M.L. and Wilhelms, S.C., 1993. WESTEX: A Numerical, One Dimensional Reservoir Thermal Model. Report 1. User's Manual, US Army Corps of Engineers, Waterways Experiment Station.

Fontane, D.G., Labadie, J.W. and Loftis, B., 1981. Optimal control of reservoir discharge quality through selective withdrawal. Water Resour. Res., 17(6): 1594-1602.

Ford, D.E. and Johnson, L.S., 1986. An Assessment of Reservoir Mixing Processes, US Army Engineer Waterways Experiment Station,Vicksburg, Miss.

Gardelin, M., Bergström, S., Carlsson, B., Graham, L.P. and Lindström, G., 2003. Climate change and water resources in Sweden — analysis of uncertainties. In: M. Beniston (Editor), Climatic Change: Implications for the Hydrological Cycle and for Water Management. Advances in Global Change Research. Springer Netherlands, pp. 189-207.

Gebre, S., Boissy, T. and Alfredsen, K., 2013. Sensitivity of lake ice regimes to climate change in the Nordic region. The Cryosphere Discuss., 7: 743-788.

Girvetz, E.H., Zganjar, C., Raber, G.T., Maurer, E.P., Kareiva, P. and Lawler, J.J., 2009. Applied Climate-Change Analysis: The Climate Wizard Tool. PLoS ONE, 4(12).

Hay, L.E., Wilby, R.L. and Leavesley, G.H., 2000. A comparison of delta change and downscaled GCM scenarios for three mountainous basins in the United States. Journal of the American Water Resources Association, 36(2): 387-397.

Henderson-Sellers, B., 1986. Calculating the surface energy balance for lake and reservoir modeling: A review. Rev. Geophys., 24(3): 625-649.

Hocking, G., Sherman, B. and Patterson, J., 1988. Algorithm for Selective Withdrawal from Stratified Reservoir. Journal of Hydraulic Engineering, 114(7): 707-719.

Imberger, J., 1982. Dynamics of Lakes, Reservoirs, and Cooling Ponds. Ann. Rev. Fluid Mech., 14: 153-187.

Imberger, J. and Fischer, H.B., 1970. Selective withdrawal from a stratified reservoir. Environmental Protection Agency, Water Quality Office, Washington, D.C., 104 pp.

Imberger, J., Thompson, R.T. and Fandry, C., 1976. Selective withdrawal from a fine rectangular tank. J. Fluid Mech., 78(03): 489-512.

Imerito, A., 2007. Dynamic reservoir simulation model DYRESM, v4.0 Science Manual. Centre for Water Research, University of Western Australia, pp. 50.

IPCC, 2007. Climate Change 2007: The Physical Science Basis. Contribution of Working Group I to the Fourth Assessment Report of IPCC ,(Available at www.ipcc.ch).

Jager, H.I. and Smith, B.T., 2008. Sustainable Reservoir Operation: Can We Generate Hydropower and Preserve Ecosystem Values? River. Res. Applic. , 24: 340–352.

Johnson, B.M., Saito, L., Anderson, M.A., Weiss, P., Andre, M. and Fontane, D.G., 2004. Effects of Climate and Dam Operations on Reservoir Thermal Structure. Journal of Water Resources Planning and Management, 130(2): 112-122.

Jones, R., 2000. Managing Uncertainty in Climate Change Projections – Issues for Impact Assessment. Climatic Change, 45(3-4): 403-419.

Killingtveit, Å. and Sæalthun, N.R., 1995. Hydrology. Hydropower Development, Volume 7, Norwegian Institute of Technology, Division of Hydraulic Engineering.

Kundzewicz, Z.W., L.J. Mata, N.W. Arnell, P. Döll, P. Kabat, B. Jiménez, K.A. Miller, T. Oki, Z. Sen and I.A. Shiklomanov, 2007. Freshwater resources and their management. In: M.L. Parry, O.F. Canziani, J.P. Palutikof, P.J.v.d. Linden and C.E. Hanson (Editors), Climate Change 2007: Impacts, Adaptation and Vulnerability. Contribution of Working Group II to the Fourth Assessment Report of the Intergovernmental Panel on Climate Change, Cambridge University Press, Cambridge, UK, pp. 173-210.

Lawrence, D. and Hisdal, H., 2011. Hydrological projections for floods in Norway under a future climate, No. 5-2011. NVE, Oslo, 47 pp.

Leppäranta, M., 1993. A review of analytical models of sea - ice growth. Atmosphere-Ocean, 31(1): 123-138.

MacKay, M.D., Neale, P.J., Arp, C.D., Domis, L.N.D.S., Fang, X., Gal, G., Jo¨hnk, K.D., Kirillin, G., Lenters, J.D., Litchman, E., MacIntyre, S., Marsh, P., Melack, J., Mooij, W.M., Peeters, F., Quesada, A., Schladow, S.G., Schmid, M., Spence, C. and Stokes, S.L., 2009. Modeling lakes and reservoirs in the climate system. Limonology and Oceanography 54(6, part 2): 2315-2329.

Marcotte, N., 1980. Thermal stratification in reservoirs of a pumped-storage power plant. In: T. Carstens and T. McClimans (Editors), Second International Symposium on Stratified Flows. Tapir, The Norwegian Institute of Technology, Trondheim, pp. 967-976.

Martynov, A., Sushama, L., Laprise, R., Winger, K. and Dugas, B., 2012. Interactive lakes in the Canadian Regional Climate Model, version 5: the role of lakes in the regional climate of North America. Tellus A, 64: 1-22.

Maurer, E.P., 2007. Uncertainty in hydrologic impacts of climate change in the Sierra Nevada, California under two emissions scenarios. Climatic Change, Vol. 82(3-4): 309-325.

Mohr, M. and Tveito, O.E., 2008. Daily temperature and precipitation maps with 1 km resolution derived from Norwegian weather observations, 13th Conference on Mountain Meteorology/17th Conference on Applied Climatology, Whistler, BC, Canada pp. 6.

Nakićenović, N. and Swart, R. (Editors), 2000. Special Report on Emissions Scenarios. A Special Report of Working Group III of the Intergovernmental Panel on Climate Change, Cambridge University Press, Cambridge, United Kingdom and New York, NY, USA, 599 pp.

Nelder, J.A. and Mead, R., 1965. A Simplex Method for Function Minimization. The Computer Journal, 7(4): 308-313.

Parker, F.L., Barry A. Benedict and Chii-ell Tsai, 1975. Evaluation of mathematical models for temperature prediction in deep reservoirs, National Environmental Research Center, Oregon, pp. 205.

Peeters, F., Livingstone, D.M., Goudsmit, G.-H., Kipfer, R. and Forster, R., 2002. Modeling 50 years of historical temperature profiles in a large central European lake. Limnol. Oceanogr., 47: 186–197.

Reed, R.K., 1977. On Estimating Insolation over the Ocean. Journal of Physical Oceanography, 7(3): 482-485.

Roeckner, E., Brokopf, R., Esch, M., Giorgetta, M., Hagemann, S., Kornblueh, L., Manzini, E., Schlese, U. and Schulzweida, U., 2006. Sensitivity of Simulated Climate to Horizontal and Vertical Resolution in the ECHAM5 Atmosphere Model. Journal of Climate, 19(16): 3771-3791.

Sahlberg, J., 2003. Physical modelling of the Akkajaure reservoir. Hydrology and Earth System Sciences, 7(3): 268-282.

Sahoo, G. and Schladow, S., 2008. Impacts of climate change on lakes and reservoirs dynamics and restoration policies. Sustainability Science, 3(2): 189-199.

Sahoo, G., Schladow, S., Reuter, J. and Coats, R., 2011. Effects of climate change on thermal properties of lakes and reservoirs, and possible implications. Stochastic Environmental Research and Risk Assessment, 25(4): 445-456.

Sahoo, G.B. and Schladow, S.G., 2010. Impacts of Climate Change on Lakes and Reservoirs Dynamics and Restoration Policies. In: A. Sumi, K. Fukushi and A. Hiramatsu (Editors), Adaptation and Mitigation Strategies for Climate Change. Springer Japan, pp. 37-55.

Saloranta, T.M. and Andersen, T., 2007. MyLake—A multi-year lake simulation model code suitable for uncertainty and sensitivity analysis simulations. Ecological Modelling, 207: 45-60.

Saloranta, T.M., Forsius, M., Järvinen, M. and Arvola, L., 2009. Impacts of projected climate change on the thermodynamics of a shallow and a deep lake in Finland: model simulations and Bayesian uncertainty analysis. Hydrology Research, 40(2-3): 234-248.

Saltveit, S.J., 2006. Økologiske forhold i vassdrag : konsekvenser av vannføringsendringer : en sammenstilling av dagens kunnskap (in Norwegian). Norges vassdrags- og energidirektorat, Oslo, 152 pp.

Samuelsson, P., Jones, C.G., Willén, U., Ullerstig, A., Gollvik, S., Hansson, U.L.F., Jansson, C., Kjellström, E., Nikulin, G. and Wyser, K., 2011. The Rossby Centre Regional Climate model RCA3: model description and performance. Tellus A, 63(1): 4-23.

Schmidlin, T.W., 2005. Lakes, Effects on Climate. In: J.E. Oliver (Editor), Encyclopedia of World Climatology. Springer, pp. 444-445.

Schneider, M.L., Wilhelms, S.C. and Yates, L.I., 2004. SELECT Version 1.0 Beta: A One-Dimensional Reservoir Selective Withdrawal Model Spreadsheet, Water Operations Technical Support Program, U.S. Army Corps of Engineers, Washington, DC, pp. 21.

Seibert, J., 2005. HBV light, version 2, user's manual, Stockholm University, Department of Physical Geography and Quaternary Geology, Stockholm.

Steen, J.E. and Stigebrandt, A., 1980. Topographical control of three-dimensional selective withdrawal. In: T. Carstens and T. McClimans (Editors), Second International Symposium on Stratified Flows. Tapir, The Norwegian Institute of Technology, Trondheim, pp. 447-455.

Stefan, H., Ambrose, R. and Dortch, M., 1989. Formulation of water quality models for streams, lakes, and reservoirs: Modeler's perspective, Department of the Army, Waterways Experiment Station, Corps of Engineers,Vicksburg, Mississippi, pp. 82.

Teutschbein, C. and Seibert, J., 2010. Regional Climate Models for Hydrological Impact Studies at the Catchment Scale: A Review of Recent Modeling Strategies. Geography Compass, 4(7): 834-860.

Thornthwaite, C.W., 1948. An Approach toward a Rational Classification of Climate. Geographical Review,, 38(1): 55-94.

TVA, 1990. BETTER: A two -dimensional reservoir water quality model, technical reference manual and user's guide, Tennessee Valley Authority, Water Resources Research Laboratory,TN.

USACE, 1986. WQRRS Water Quality for River-Reservoir Systems, User's manual. United States Army Corp of Engineers, Hydrologic Engineering Center. October 1978, revised 1986., pp. 380.

van der Linden P. and Mitchell, J.F.B. (Editors), 2009. ENSEMBLES: Climate Change and its Impacts: Summary of research and results from the ENSEMBLES project, Met Office Hadley Centre, FitzRoy Road, Exeter EX1 3PB, UK. , 160 pp.

Wetzel, R.G., 2001a. Fate of heat, Limnology: Lake and river ecosystems. Academic Press, San Diego, Ca., pp. 71-92.

Wetzel, R.G., 2001b. Water movements, Limnology: Lake and river ecosystems. Academic Press, San Diego, Ca., pp. 93-128.

Table 1. Salient features of the three reservoir sites

Physical Characteristics	**Follsjoe**	**Tesse**	**Alta**
Geographic Location	N 62° 57' 56" E 09° 06' 51"	N 61° 46' 08" E 08° 57' 25"	N 69° 41' 40" E 23° 49' 36"
Surface Area (km^2)	6.79	12.6	6.75
Maximum Depth (m)	60.8	70.4	96.8
Mean depth (m)	29.5	23.6	20.4
Reservoir Volume (Million m^3)	200	297	138
Highest Regulated Water Level (m)	420	854.4	265
Lowest Regulated Water Level (m)	375	842	200
Catchment Area (km^2)	575	380	5940
Mean annual inflow (Million m^3)	903	262	2250
Installed capacity (MW)	130	16	150
Annual Energy production (GWh)	805	90	665
Outlet levels (m)	395 / 375	837m	255 / 183

Table 2. Parameters optimised in the three reservoir models

No.	Parameters / Coefficients	Ranges and references*	Optimal/selected values		
			Alta	Follsjoe	Tesse
1	$^{+}a_k$	> 0	3.127	0.097	0.139
2	$^{+}W_{str}$	0 - 1	0.66	1.00	1.00
3	$^{+}$k1	2 - 6	2.57	4.52	5.35
4	Albedo_ ice	0.10-0.60a,b	0.20	0.25	0.27
5	Albedo_snow	0.40-0.95a,b,c	0.60	0.77	0.65
6	$^{\$}\lambda$-water ($m^{-1}$)	0.8-1.3d,0.32-0.62e	1.21	0.58	1.2
7	$^{\$}\lambda$-ice ($m^{-1}$)	2.5-3.0f,0.6-3.4g, 3.5h	1.37	1.13	1.7
8	$^{\$}\lambda$-snow ($m^{-1}$)	10-20g, 15f ,25h,7-30i	22	18	24

$^{+}$ a_k is the coefficient in the diffusivity equation, $Kz = a_k (N^2)^{-0.43}$, Wstr is the wind sheltering coefficient, k1is the coefficient in the equation $\delta = k1\sqrt{q/N}$ for withdrawal thickness.

$^{\$}$ λ is the light attenuation coefficient

* a- Zdorovennova et al. (2013); b- Arst et al. (2008); c- Prowse et al. (1990); d- Saloranta and Andersen (2004); e-Stefan et al. (1995); f – Wright (1964); g- Erm et al. (2010); h-Pang and Stefan (1996); i-Jaatinen et al. (2010

Table 3. Model Performance for vertical temperature profiles

Reservoir	**Run period**	***Performance criteria**			
		MBE	**MAE**	**RMSE**	**NSE**
Alta	Full period	0.33	0.68	1.13	0.95
	Calibration	0.30	1.00	1.55	0.93
	Verification	0.36	0.37	0.48	0.88
Follsjoe	Full period	0.11	0.61	0.64	0.94
	Calibration	0.07	0.65	0.82	0.92
	Verification	0.15	0.57	0.77	0.95
Tesse	Full period	0.02	0.60	0.77	0.97
	Calibration	-0.03	0.60	0.78	0.97
	Verification	0.07	0.59	0.76	0.98

*MBE=Mean Bias Error, MAE=Mean Absolute Error, RMSE=Root Mean Squared Error, NSE=Nash Sutcliffe Efficiency

Table 4. Model Performance for withdrawal temperature

Reservoir	Run period	Performance criteria			
		MBE	**MAE**	**RMSE**	**NSE**
Alta	Full period	0.24	0.87	1.30	0.94
	Calibration	0.23	0.81	1.26	0.94
	Verification	0.25	0.93	1.35	0.93
Follsjoe	Full period	0.05	0.77	1.02	0.94
	Calibration	-0.15	0.70	0.97	0.94
	Verification	0.25	0.84	1.07	0.93

Table 5. Results of HBV model calibration and verification in terms of Nash-Sutcliffe Efficiency (NSE)

	Soeya near Follsjoe	Saelatunga near Tesse	Alta
Calibration	0.73	0.80	0.86
Validation	0.61	0.79	0.82

Table 6. Summary of expected changes in mean ice phenology and maximum ice thickness for the four scenarios considered. Also shown are mean simulated values for the baseline period

Reservoir	Scenarios	Freeze-up date	Break-up date	Max. Ice thickness (cm)	Max. Snow depth (cm)
Alta					
	Baseline	18-Nov	Jun-12	91	21
	Had4170	6	-10	-13	-5
	Ech4170	9	-6	-5	-3
	Had7100	11	-16	-22	-9
	Ech7100	14	-14	-16	-5
Follsjoe					
	Baseline	19-Dec	23-May	57	13
	Had4170	20	-30	-34	-7
	Ech4170	27	-31	-36	-8
	Had7100	42	-38	-43	-10
	Ech7100	42	-47	-45	-11
Tesse					
	Baseline	25-Nov	29-May	78	18
	Had4170	9	-12	-18	-6
	Ech4170	11	-7	-9	-3
	Had7100	18	-18	-29	-8
	Ech7100	16	-13	-17	-5

Table 7. Comparison of mean ice phenology and maximum snow depth and ice thickness derived from using the delta-change (DC) approach and the direct method (DM). Baseline means for ice phenology are given in julian dates (Jan 01 = 1), and thicknesses are given in cm.

	Mean for baseline			Future Changes			
Parameter	**Obs.**	**Had**	**Ech**	**Had7100 (DC)**	**Had7100 (DM)**	**Ech7100 (DC)**	**Ech7100 (DM)**
Freeze-up date	352	349	356	36	36	41	28
Break-up date	144	145	146	-42	-42	-50	-31
Max. Ice thickness	57	63	62	-43	-42	-45	-42
Max. Snow depth	13	16	14	-10	-12	-11	-9

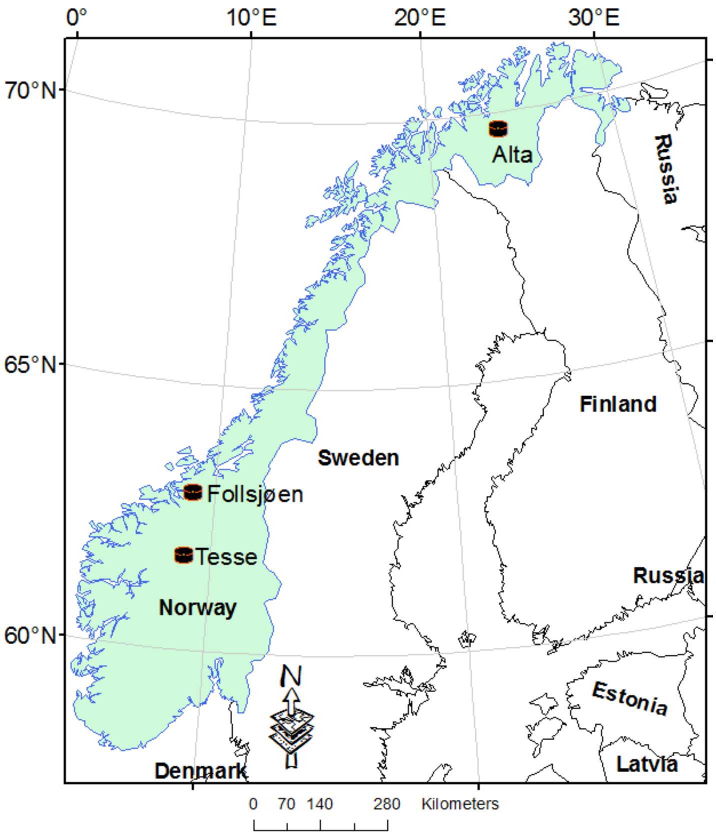

Fig. 1. Location of the three study reservoir sites

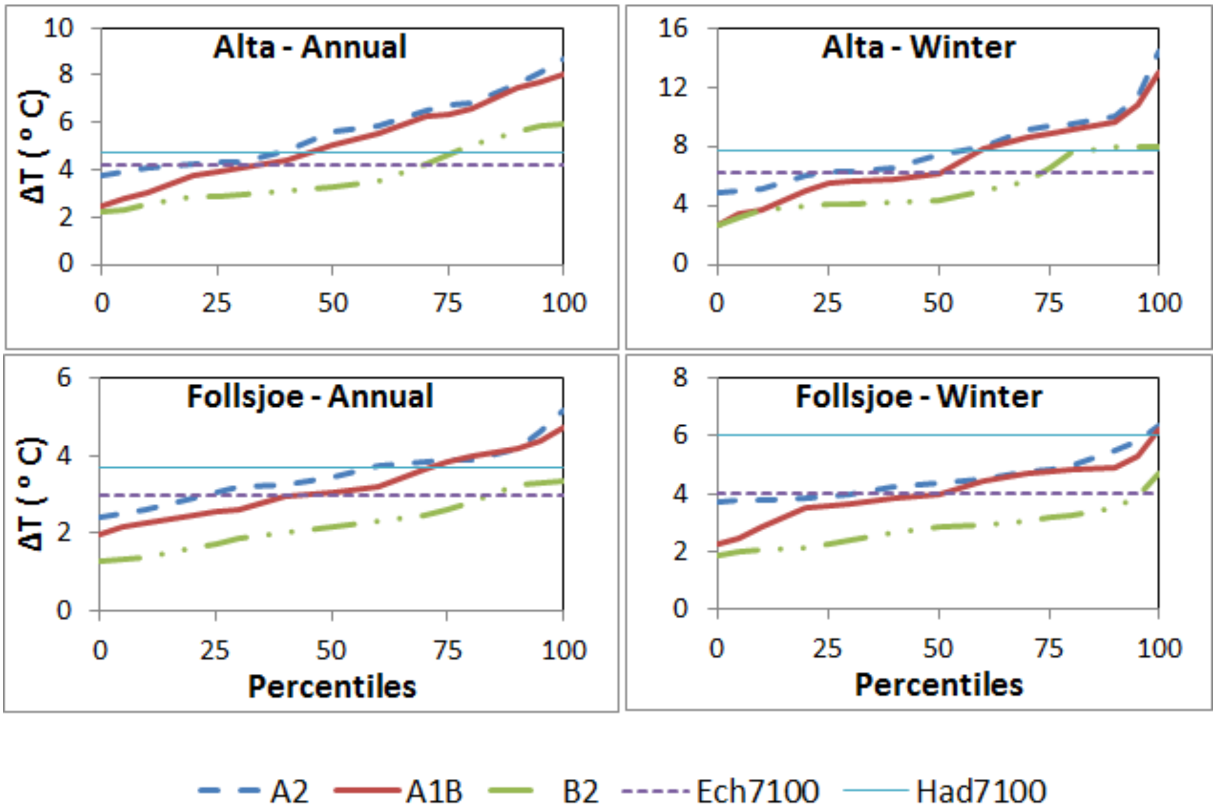

Fig. 2. Comparison of ensemble simulations of 16 GCMs and 3 different SRES emissions scenarios (A2, A1B, B1) from globally downscaled data at ~ 50km resolution (Girvetz et al., 2009), and what we have used in this study (Ech7100 and Had7100). The control period is 1961-1990, and the future period is 2071-2100.

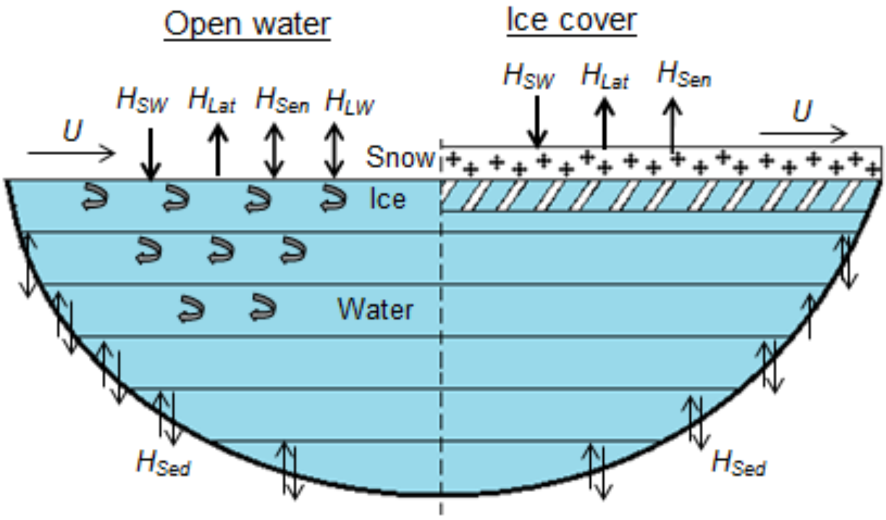

Fig. 3. Figure showing the heat budget during the open water and ice covered season (H_{SW} = Short-wave radiation, H_{Lat} = latent heat flux, H_{Sen}= Sensible (Convective) heat flux, H_{Lw} = Long-wave radiation, and H_{Sed} = sediment heat flux, U = wind speed)

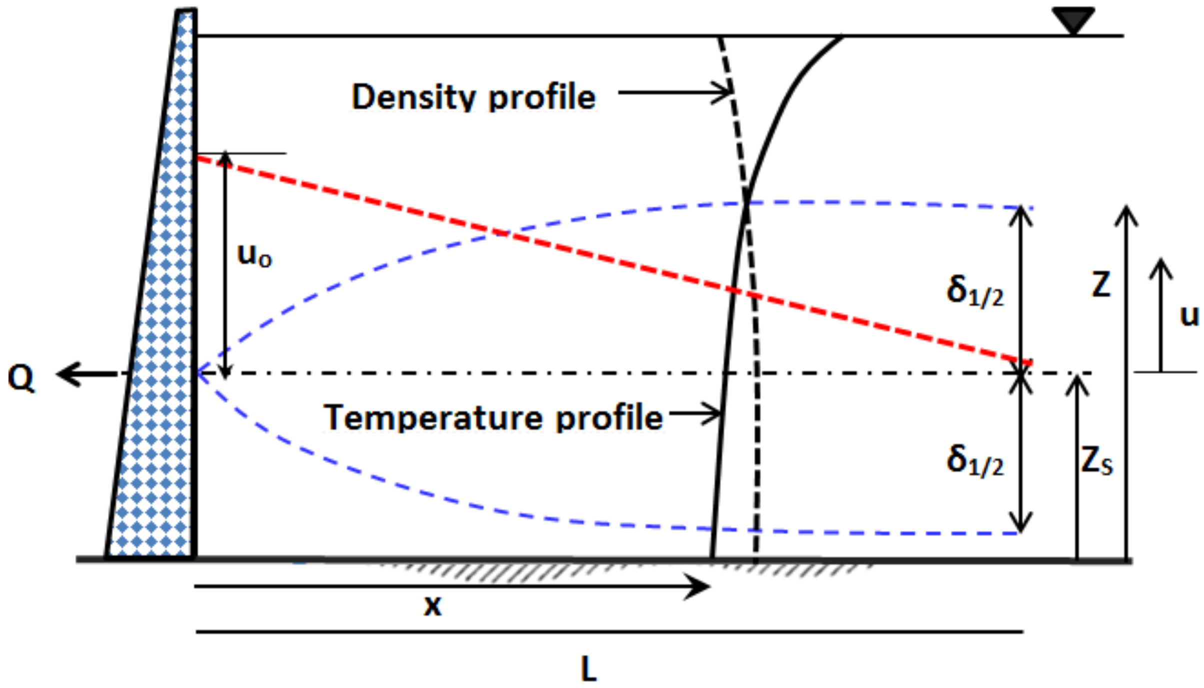

Fig. 4. Withdrawal from a stratified reservoir to illustrate the description of equations used

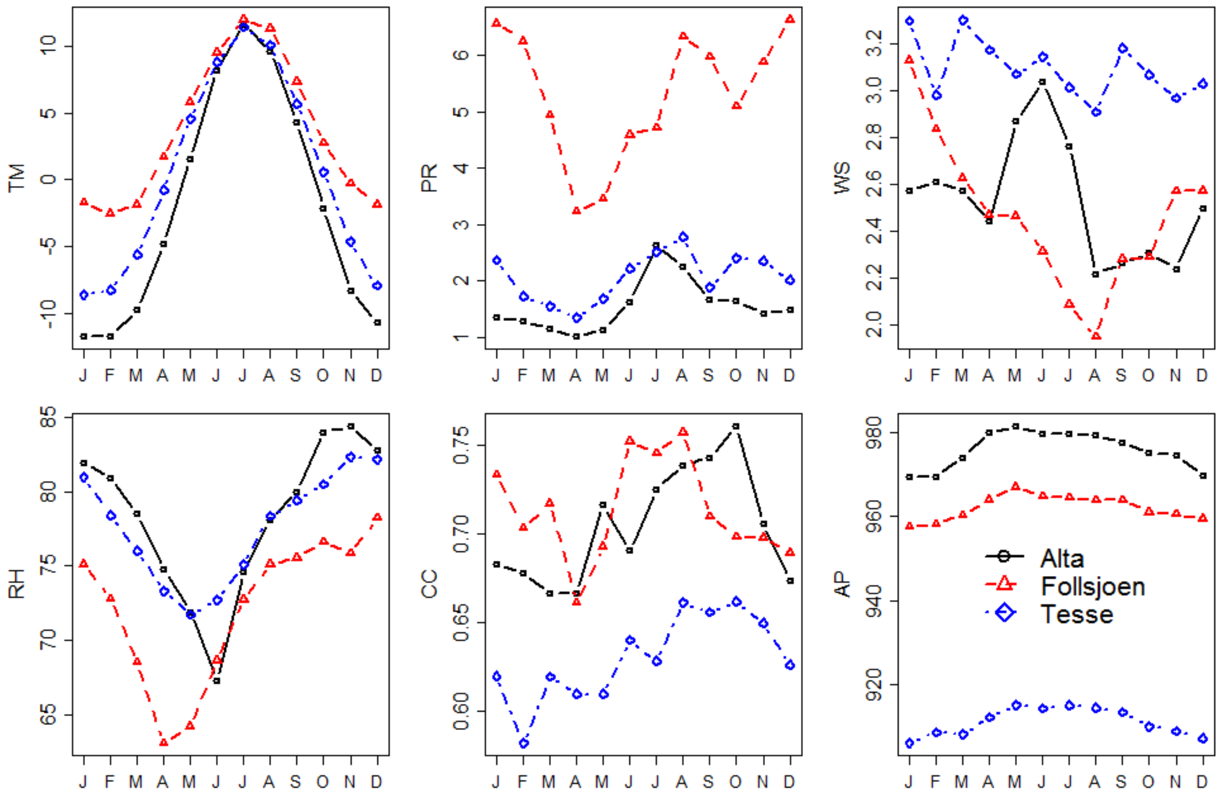

Fig. 5. Forcing data for baseline study of the three reservoirs as mean monthly values (TM=air temperature, ºC; PR=precipitation, mm/day; WS =wind speed, m/s; RH=relative humidity, %; CC=cloud cover (0 to 1); AP=air pressure, hPa)

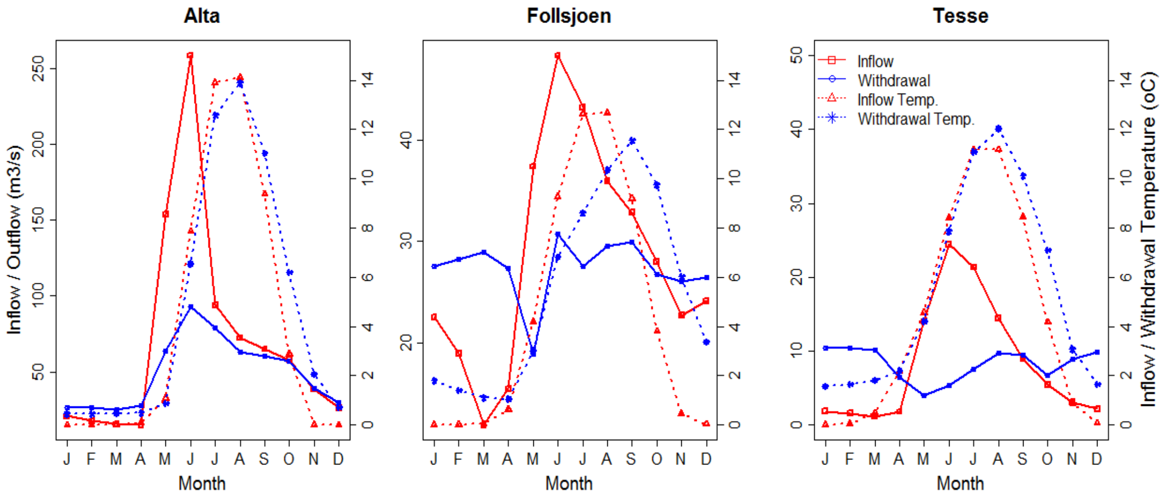

Fig. 6. Monthly mean inflow and water withdrawal in m3/s as well as inflow and withdrawal temperatures in °C for the three reservoir sites

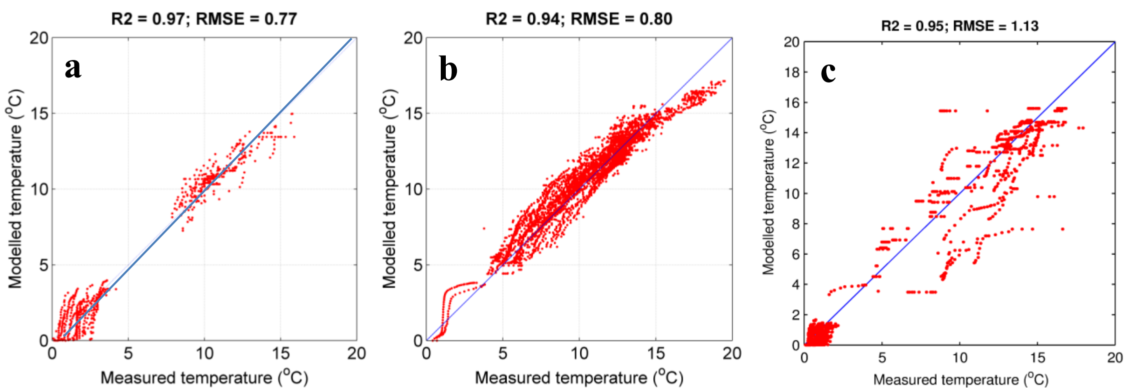

Fig. 7. Comparison of observed and simulated vertical water temperature profiles for **a)** Tesse Reservoir, **b)** Follsjoe Reservoir, and **c)** Tesse Reservoir; also shown are the Root Mean Squared Error (RMSE) and the Nash-Sutcliffe efficiency (R^2), and the 45° line.

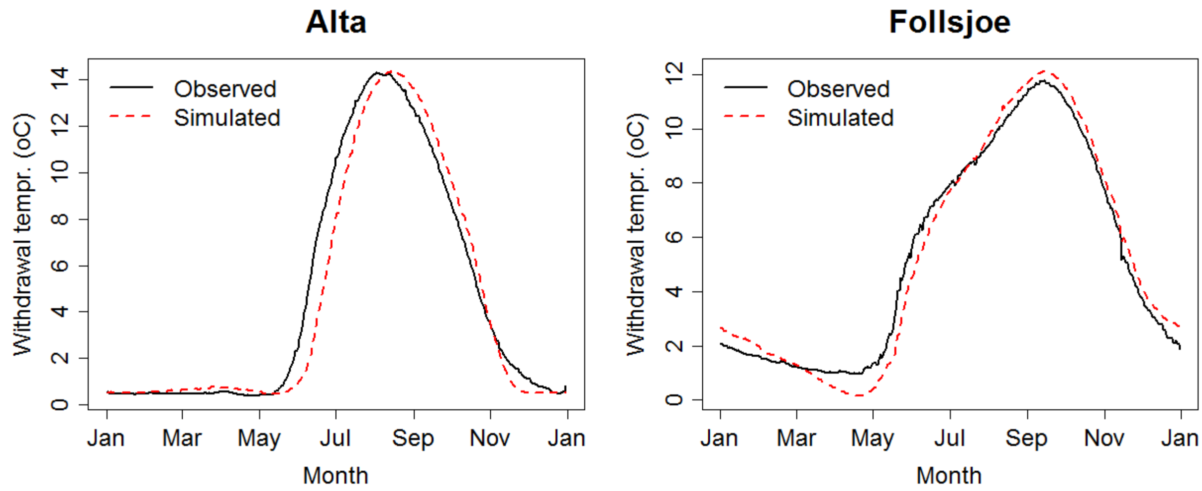

Fig. 8. Validation of simulated withdrawal temperatures for Alta and Follsjoe Reservoirs (shown are mean daily values over the simulation period)

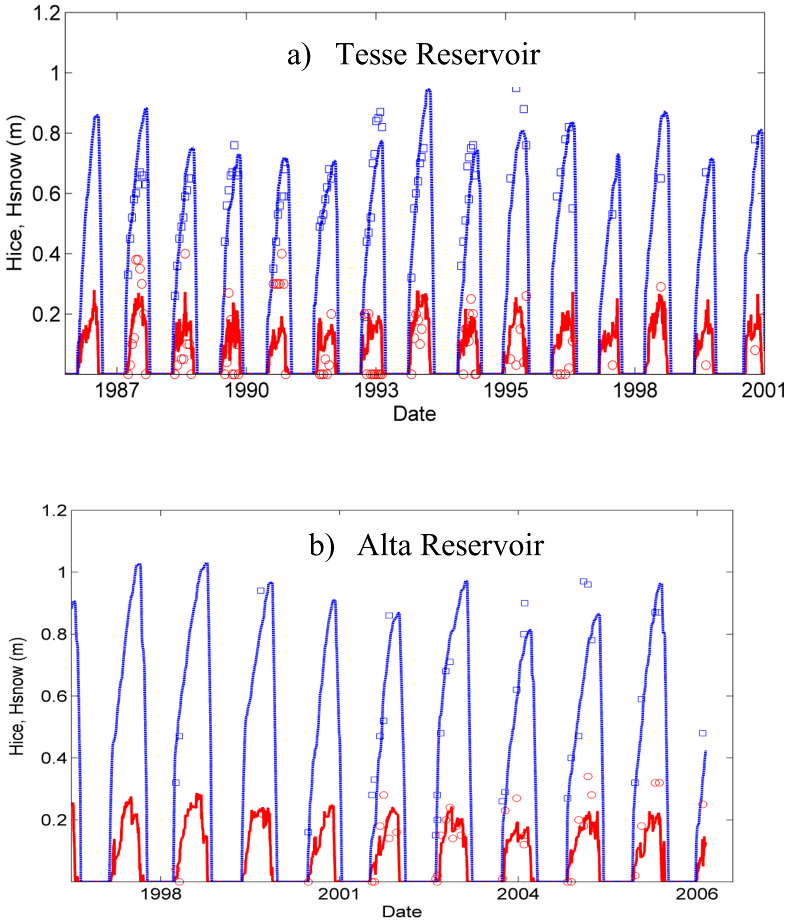

Fig. 9. Observed and simulated total ice thickness and snow depth for a) Tesse and b) Alta Reservoirs

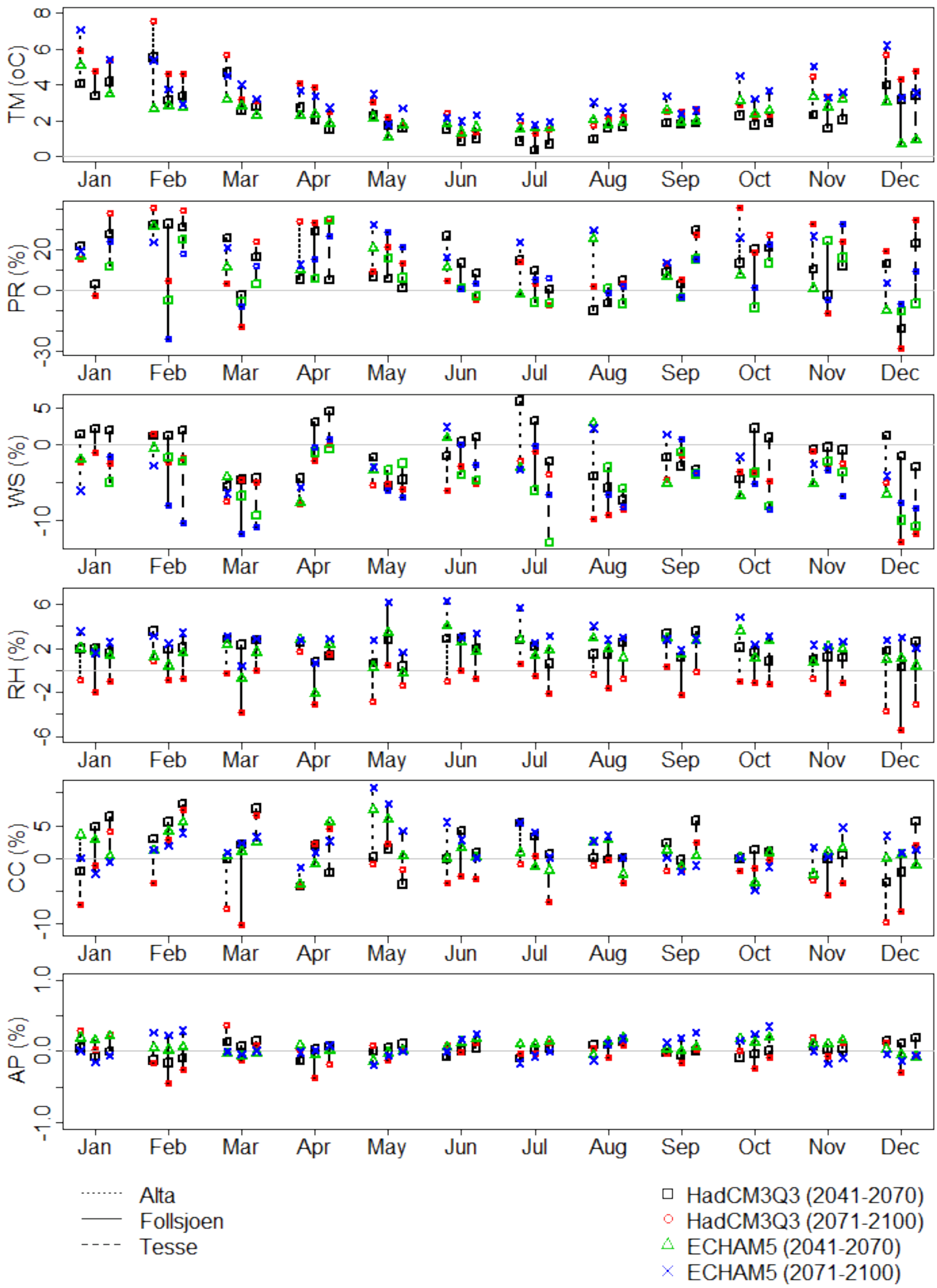

Fig. 10. Mean monthly climate change signals from the two downscaled GCMs and the two future time periods used in this study (TM=air temperature, PR=Precipitation, WS=wind speed, RH=relative humidity, CC=cloud cover, AP=air pressure)

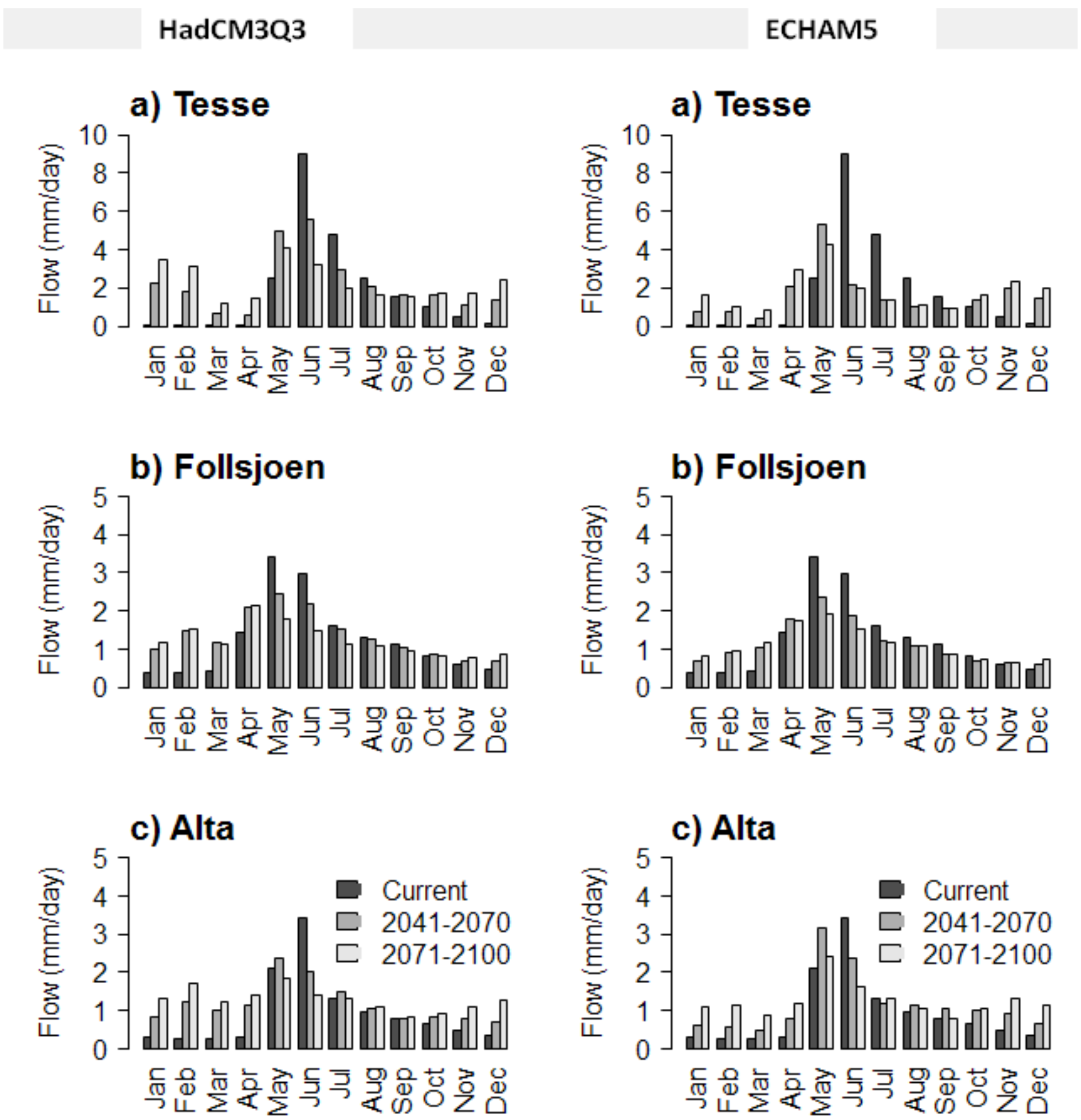

Fig. 11. Comparison of model simulations (mean monthly runoff) for the current period and two future periods (2050s and 2080s) resulting from dynamically downscaled HadCM3Q3 (left) and ECHAM5 (right) GCM forcings for IPCC emissions scenario A1B

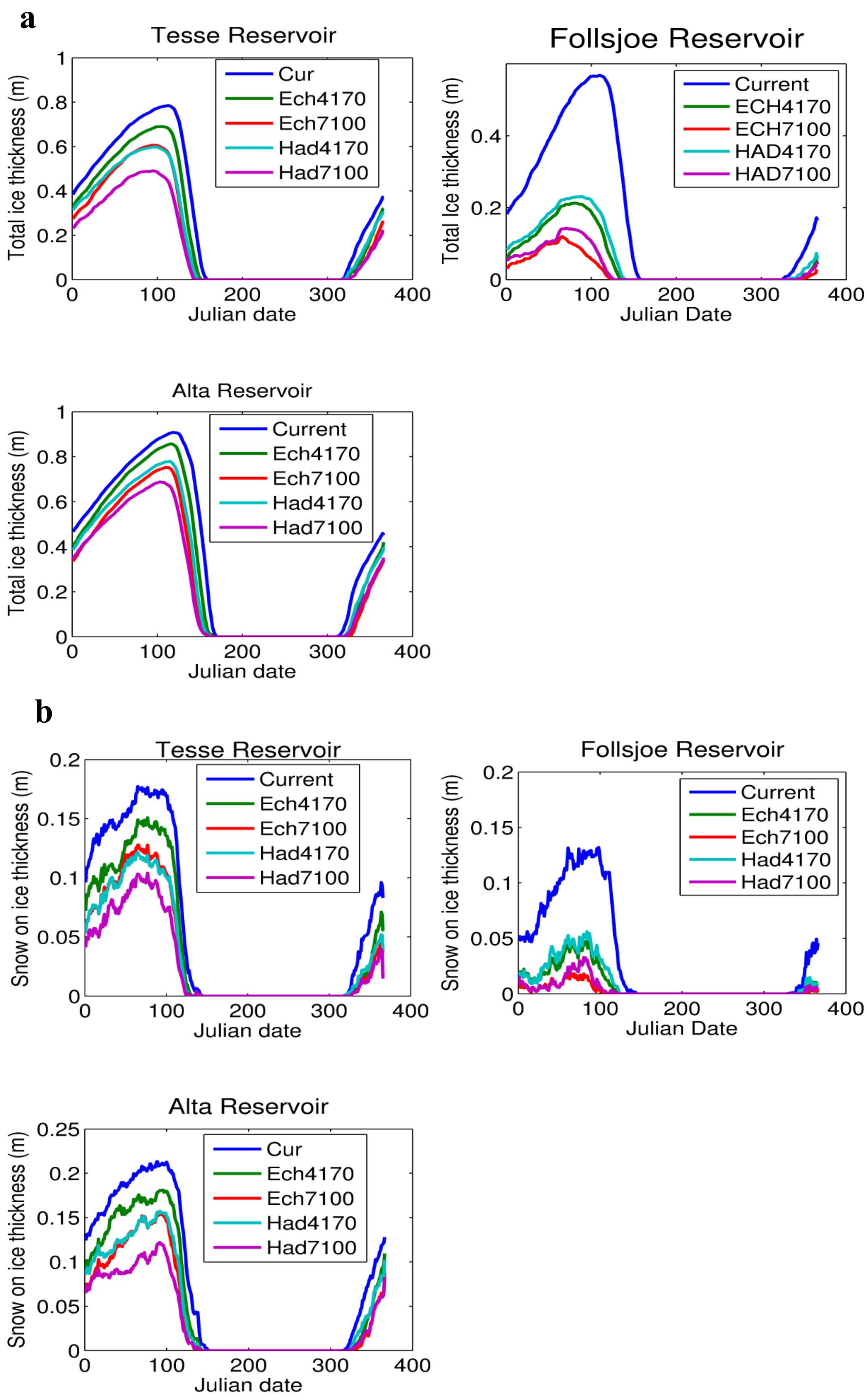

Fig. 12. Mean changes in a) ice thickness, and b) snow-on-ice thickness between the current period and the four future scenarios

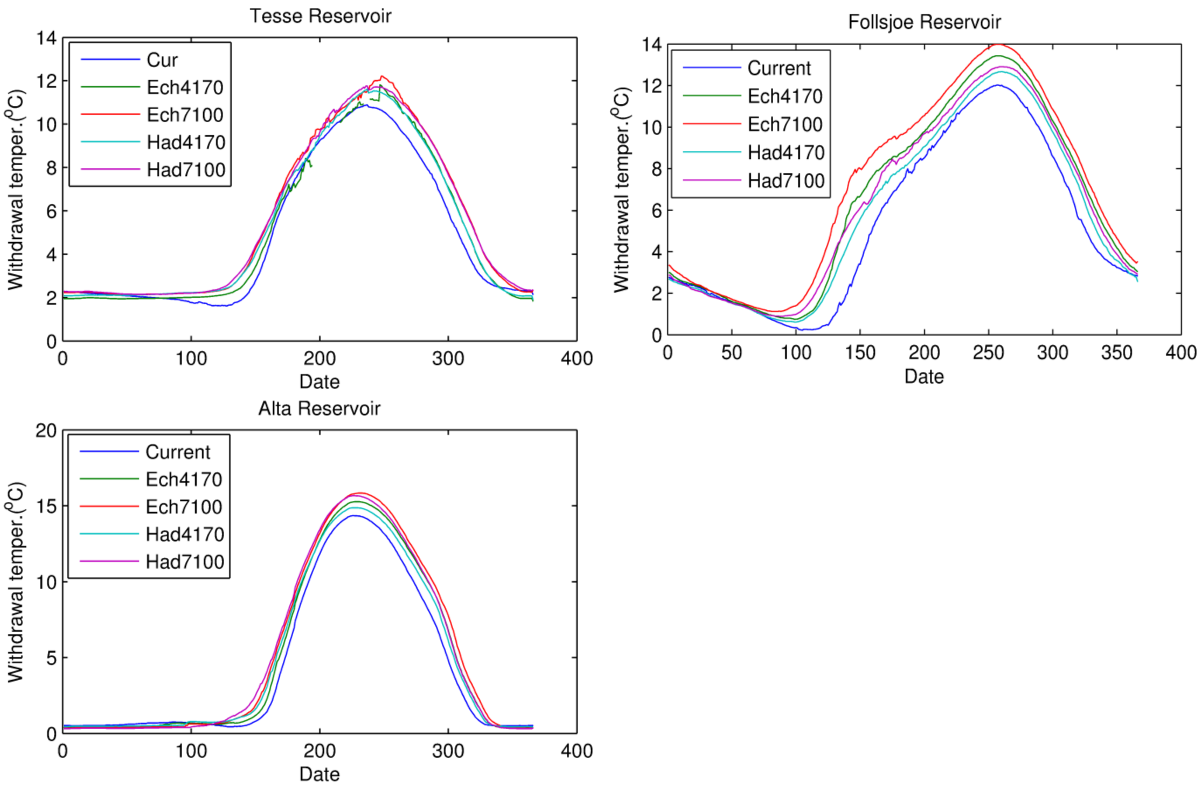

Fig. 13. Mean changes in withdrawal temperatures between the current period and the four future scenarios

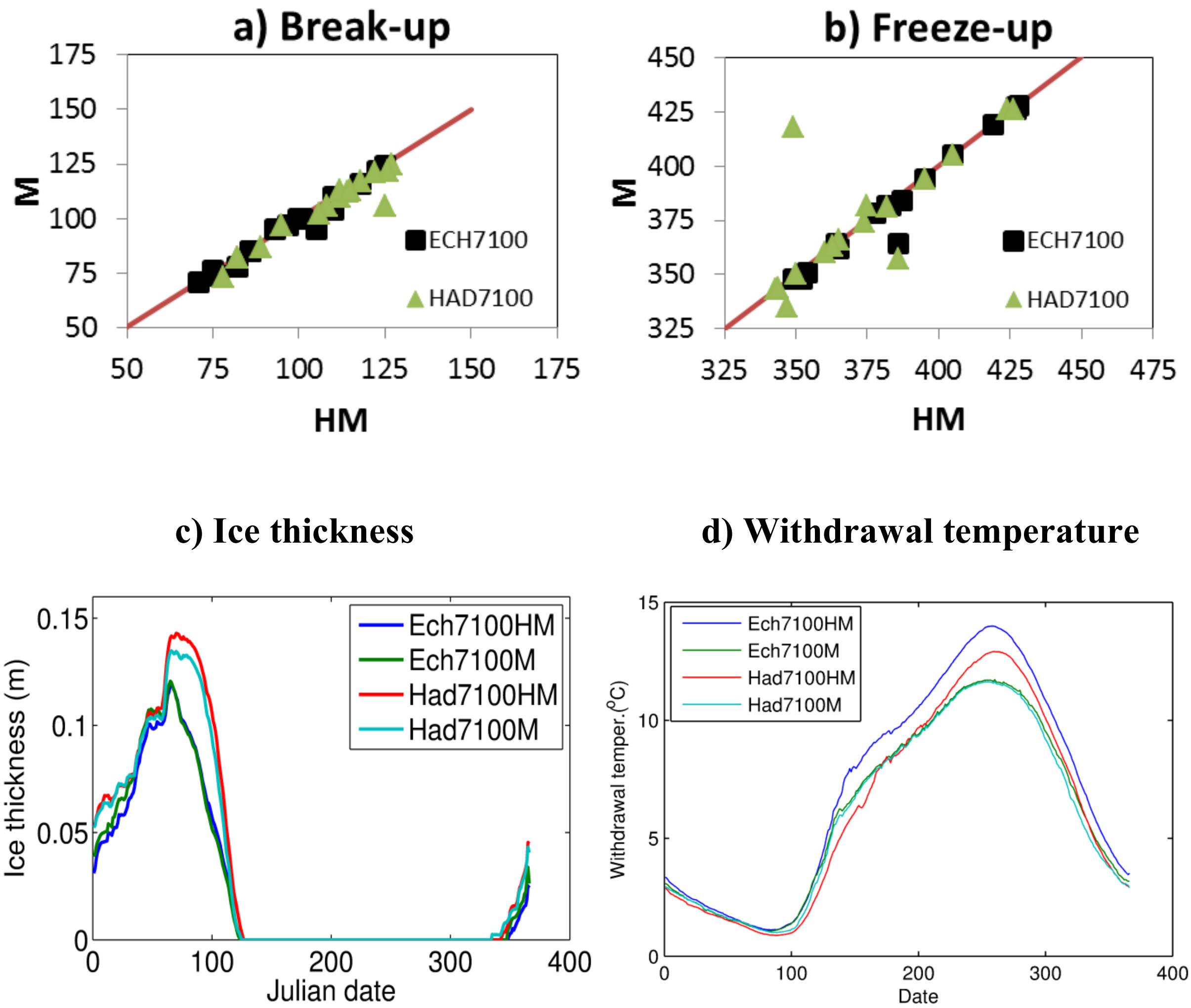

Fig. 14. Sensitivity to hydrological forcing of a) break-up, b) Freeze-up, c) Ice thickness, and d) Withdrawal temperature, M and HM in axis labels of a) and b); and in the legends of c) and d) represent respectively only changes in meteorological forcing (M), and changes in both meteorological and hydrological forcings (HM)

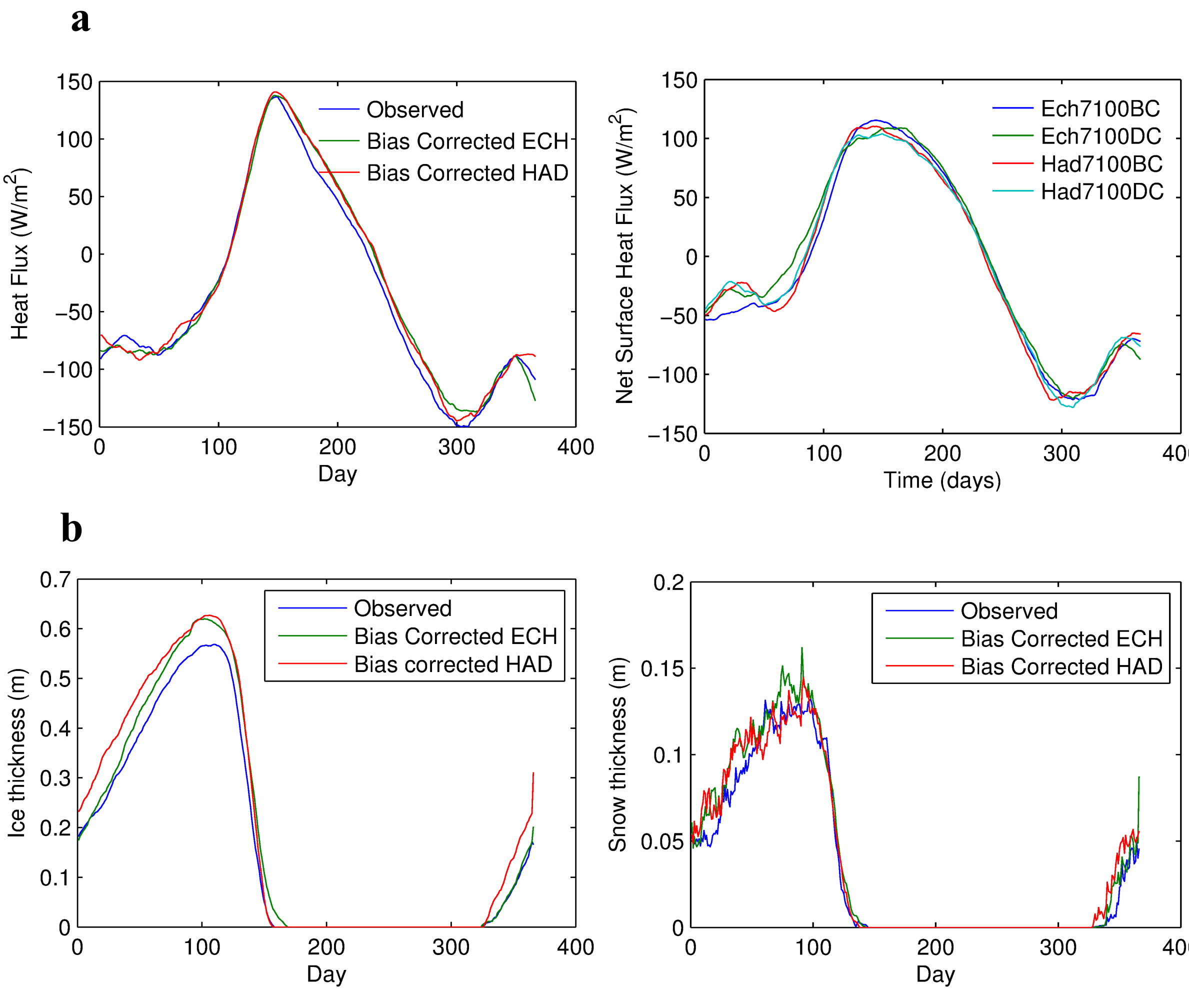

Fig. 15 a) Net surface heat fluxes for the baseline and future periods using observed data as baseline (delta-change approach) and RCM bias-corrected meteorological forcings for Follsjoe reservoir ; **b)** Comparison of ice cover (left), and snow depth (right) evolution on Follsjoe Reservoir using observed meteorological data and bias-corrected data derived from Had7100 and Ech7100

a)

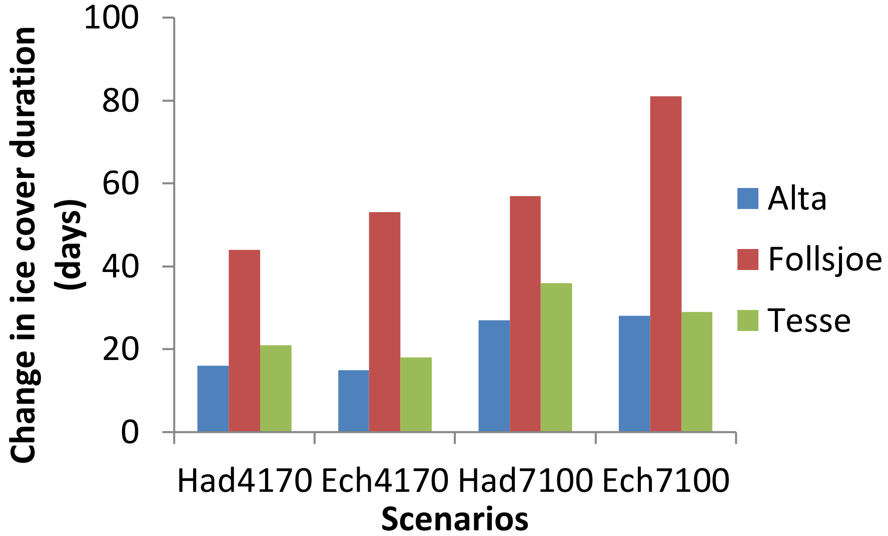

b)

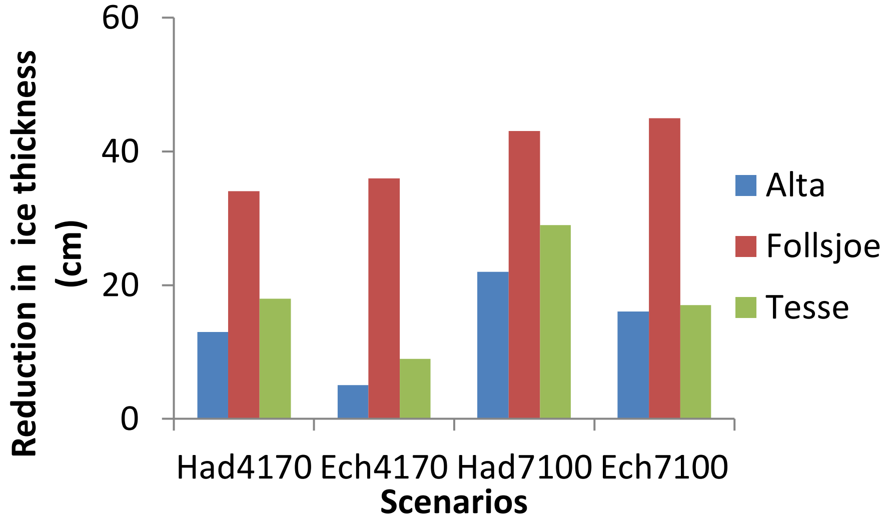

Fig. 16. Future changes in ice cover duration (a) and reduction in ice thickness (b) for the three reservoirs